Master Thesis in Geographical Information Science nr 207

Mapping forest felling activities in Latvia from Sentinel-2 satellite imagery using machine learning

Gintars Krumins

2026

Department of Earth and Environmental Sciences

Lund University
Sölvegatan 12

S-223 62 Lund

Sweden

Gintars Krumins (2026). Mapping forest felling activities in Latvia from Sentinel-2 satellite imagery using machine learning

Master degree thesis, 30 credits in Master in Geographical Information Science

Department of Earth and Environmental Sciences, Lund University

Mapping forest felling activities in Latvia from Sentinel-2 satellite imagery using machine learning

---

Gintars Krumins

Master thesis, 30 credits, in Geographical Information Sciences

Lars Eklundh

Department of Earth and Environmental Sciences, Lund University

Acknowledgements

I would like to thank my supervisor, Lars Eklundh, for his expert guidance, continuous support, and mentorship throughout the development of this thesis. I would also like to thank Latvian State Forests for providing the data that made this research possible.

Abstract

The thesis develops and evaluates Random Forest (RF) machine learning classification framework for detecting clear-cut forest felling events in Sentinel-2 multispectral satellite data. While RF classification has been widely used for forest monitoring studies, its performance assessments for operational clear-cut detection under Latvian forests remains insufficiently studied. Model training was conducted using four study areas within Latvian State Forests districts. For each study area, cloud-masked Sentinel-2 scene was selected to represent pre-felling (2018) and post-felling (2024) conditions, resulting in a multi-temporal datasets with acquisition dates varied between study areas. Median spectral reflectance features were derived using historical felling records. Model evaluation included two testing methods: internal testing on the training areas to assess performance on data seen by RF model during training (self-testing) and testing on a separate, fifth forest district, which was not used in the model training. Metrics such as overall accuracy, user accuracy (precision), producer accuracy (recall) and F1 score (balanced measure of precision and recall) were calculated to assess model performance.

Results indicated that the model classifications achieved over 70 % user and producer accuracies in an unseen area by the model, with overall accuracy exceeding 95 %. The analysis included an evaluation of the contribution of individual Sentinel-2 bands. Spectral bands in the visible and shortwave infrared regions were identified as the most important for distinguishing felled and non-felled forest compartments. The analysis included addition of vegetation indices, which increased accuracies by 1-4 %. Misclassifications were primarily associated with sanitary fellings and cloud-affected pixels.

The results of this thesis show that an RF model trained on Sentinel-2 data is capable of detecting clear-cut felling events in Latvian forests. The study highlights the importance of spectral band selection, vegetation indices and robust model validation, providing additional capabilities in forest monitoring in semi-boreal regions.

Keywords

Latvia, Sentinel-2, Random Forest, remote sensing, GIS, forest felling detection, vegetation indices, spectral signature analysis.

Kopsavilkums

Maģistra darba mērķis bija izpētīt Random Forest (RF) mašīnmācīšanās algoritma potenciālu noteikt galvenās cirtes Sentinel-2 satelītuzņēmumos. Pētījumā tika analizēta algoritma spēja atšķirt galvenās cirtes no nenocirstajām teritorijām Latvijā, balstoties uz tālizpētes datiem. Modeļa apmācībai tika izmantotas četras paraugteritorijas, Latvijas valsts mežu iecirkņi, iegūstot mediāno spektrālo statistiku no vēsturiskajiem cirsmu datiem pirms (2018.g.) un pēc ciršanas (2024.g.). Modeļa novērtēšana ietvēra gan pašpārbaudi apmācību teritorijās, gan validēšanu atsevišķā, piektajā meža iecirknī, kas netika izmantots modeļa apmācīšanā. Lai novērtētu modeļa veiktspēju, tika pielietotas vairākas precizitātes, tostarp F1 rādītājs.

Modeļa rezultāti sasniedza vairāk nekā 70 % precizitāti cirsmu un necirsto meža nogabalu klasificēšanā, savukārt kopējā klasificēšanas precizitāte pārsniedza 95 %. Analīzē tika izvērtēta Sentinel-2 spektrālo joslu nozīme. Redzamās un īsviļņu infrasarkanā spektra joslas tika identificētas kā vissvarīgākās, lai atšķirtu nocirstās un nenocirstās meža teritorijas. Analīzē tika iekļauta arī veģetācijas indeksu izmantošana, kas nodrošināja papildu precizitātes uzlabojumus. Modeļa kļūdu iemesli galvenokārt tika saistīti ar sanitārajām cirsmām un mākoņu ietekmētajiem pikseļiem.

Darba rezultāti liecina, ka RF modelis, apmācīts uz Sentinel-2 datiem, ir spējīgs identificēt galvenās cirtes Latvijas mežos. Pētījumā tika uzsvērta spektrālo joslu izvēle, veģetācijas indeksu izmantošana un validēšana modelim nezināmā teritorijā, sniedzot papildu iespējas meža monitoringa veikšanai teritorijās, kur sastopami gan skujkoki, gan lapu koki.

Table of Contents

Acknowledgements iv
Abstract iv
Keywords v
Kopsavilkums v
Table of Contents vi
List of Tables vii
List of Figures viii
List of Abbreviations ix
1. Introduction 1
2. Theoretical background 5
2.1. Remote sensing for forest management 5
2.2. Sentinel-2 data for forest monitoring 6
2.3. Forest felling practices in Latvia 8
2.4. Machine learning techniques in remote sensing-based forest analysis 11
2.5. Vegetation indices used for forest monitoring and classification 12
3. Methods and material 15
3.1. Study areas 15
3.2. Data 17
3.3. Methods description 18
4. Results 23
4.1. Band Importance 23
4.2. Performance of the Random Forest model 24
4.3. Classification patterns and sources of misclassification 26
4.4. Vegetation indices and their effectiveness in detecting clear-cut felling 32
5. Discussion 35
6. Conclusions 41
References 43
Appendices 49

List of Tables

Table 1. Sentinel-2 spectral bands and characteristics.

Table 2. Machine learning algorithm types.

Table 3. Examples of structure-oriented vegetation indices.

Table 4. Examples of pigment-oriented vegetation indices.

Table 5. Examples of water sensitive vegetation indices.

Table 6. Sentinel-2 imagery acquisition details by forest district.

Table 7. Description of Random Forest classification report metrics.

Table 8. Random Forest model classification accuracy metrics.

Table 9. Random Forest classification by dominant tree species in forest compartments.

Table 10. Random Forest model classification accuracy metrics when sanitary fells combined with clear-cuts.

List of Figures

Figure 1. Felling area indicated in tree felling license by type of felling, year 2023.

Figure 2. Felling stock volume indicated in tree felling license by type of felling, year 2023.

Figure 3. Locations of study areas.

Figure 4. Red visible band (band 4) reflectance change (%) based on Sentinel-2 Imagery from 2018 to 2024.

Figure 5. Sentinel-2 band importance scores for forest felling detection.

Figure 6. Sentinel-2 band average spectral reflectance change (%) due to forest felling.

Figure 7. Area of well-performing fell classification in Skaistkalne district.

Figure 8. Area of low classification accuracy in Skaistkalne district.

Figure 9. Median spectral difference (2018-2024) by classification outcome.

Figure 10. Distribution of fell classification accuracy by forest compartment size.

Figure 11. Overestimated fellings near clouds – Skaistkalne district.

Figure 12. Random Forest model overclassification distribution by felling type.

Figure 13. Misclassified clear-cut fells due to sanitary felling in Skaistkalne district.

Figure 14. Importance scores of Sentinel-2 bands and vegetation indices for forest felling detection.

Figure 15. Random Forest model classification accuracy metrics with and without vegetation indices in model self-testing.

Figure 16. Random Forest model classification accuracy metrics with and without vegetation indices in unseen area testing.

List of Abbreviations

AI	Artificial Intelligence
GIS	Geographic Information Systems
LSF	Latvian State Forests
ML	Machine learning
NDMI	Normalized Difference Moisture Index
NDVI	Normalized Difference Vegetation Index
NIR	Near-Infrared
RF	Random Forest
SCL	Scene Classification Layer
SWIR	Shortwave Infrared
VARI	Visible Atmospherically Resistant Index

1. Introduction

The forest is a key element of the Latvian landscape and natural environment. In 2025 forest land covered around 3.3 million hectares, including both state-owned and privately owned forests, accounting for 51% of the country's territory (Latvian Forest Development Fund, 2025). Latvia's forests are diverse, with variations in species composition, structure and distribution across different regions. Pine and spruce species dominate the forests, covering more than a half of the total forested area (Laiviņš, 2018). Given the extent of forested land, effective monitoring of forest felling is essential for sustainable forest management, as it enables informed decision-making and supports the tactical planning of forestry activities across large and often remote areas.

Latvian state forest management planning operates at three levels: long-term, tactical, and spatial (activity) levels (Latvian State Forests, 2024):

- Long-term planning focuses on strategic objectives, such as ensuring a sustainable supply of wood products for the national economy.
- Tactical planning involves determining wood extraction volumes, road reconstruction, and other mid-term operational goals.
- Spatial (activity) planning addresses site-specific activities at the operational level, for example, felling activities.

Forest logging is a key component of sustainable forest ecosystem management and planning. Although logging operations in Latvia are typically well-documented through forest inventory data and detailed harvester records, these sources do not fully capture all historical logging activities. Remote sensing data can help identify undocumented logging operations and provide automated, repeatable and timely detection of forest cover changes in future. To complement existing datasets and improve the scalability of forest monitoring systems, there is increasing interest in leveraging remote sensing and machine learning (ML) to detect and map felling events directly from satellite imagery. Sentinel-2, with its high spatial and temporal resolution and open-access, presents a valuable data source for this purpose. By applying advanced ML models to Sentinel-2 data, this research demonstrates how satellite-based monitoring can support verification of reported harvesting activities, improve transparency, and enhance large-scale forest management and planning.

Sentinel-2 satellite data, widely recognized for its high-resolution optical imagery, is increasingly adopted in vegetation-related applications, including land cover mapping, vegetation condition monitoring and disturbance detection (Lewińska et al., 2024). Multispectral Sentinel-2 satellite system holds great potential due to its high spatial resolution up to 10m, 13 spectral bands spanning the visible, near-infrared (NIR), and shortwave infrared (SWIR) regions and its short revisit time of less than 5 days in Europe. Sentinel-2 data have demonstrated strong potential for multiple forest management tasks, such as mapping different forest attributes and dynamics at large spatial scales (Fassnacht et al., 2024).

With the advancements in artificial intelligence (AI) techniques, particularly ML, the ability to detect forest parameters has become more precise and effective. The integration of Sentinel-2 data with Geographic Information Systems (GIS) and ML algorithms offers promising opportunities for the remote identification of forest management activities. However, the performance of these methods still requires validation under specific operational conditions, which motivates this study.

One of the widely used ML algorithms in remote sensing is Random Forest (RF) classifier introduced earlier. It is a supervised ML classifier that has been used in different remote sensing solutions, for example, to reduce the number of dimensions of hyperspectral data or identify the most relevant multisource remote sensing and geographic data (Belgiu & Drăguţ, 2016).

While this algorithm demonstrated high accuracy in different remote sensing studies, most applications have focused on specific vegetation types or regions outside Latvia, highlighting a research shortage in the application of RF to local forest management. In Latvia, several attempts have been made to monitor forest conditions using Sentinel data, such as detecting tree cuts in Sentinel-1 data (Cimdiņš, 2018), biomass growth and carbon balance modelling (Silava, 2025) and identifications of potential damages in spruce stands caused by bark beetles (Latvian state forests, 2025). Despite these efforts, studies applying RF specifically for operational forest management in Latvia remain limited.

Another reason for this study is that traditional forest inventory and historical logging records, especially in private forest sector, have failed to capture all past felling activities. In some cases, large forest companies that purchase forest areas from private owners may not know when or how extensive previous felling operations were. Therefore, accurate information on past felling activities is needed for effective forest management and planning.

The main goal of this project is to apply a functional ML algorithm that can identify clear-cut forest felling events from Sentinel-2 imagery, which can help improve forest management and planning. The study will focus on Latvia, with model training conducted on four reference areas within Latvian State Forest districts, selected for their rich training data. The research integrates Sentinel-2 satellite data, historical forest felling records, and machine learning techniques within a GIS-based processing environment. The Random Forest algorithm is employed to classify felling events based on spectral information derived from Sentinel-2 bands. By assessing the contribution of individual spectral bands and additional vegetation indices, the study aims to improve the accuracy and reliability of remote sensing-based forest disturbance detection.

Specific research questions are:

- How do different Sentinel-2 bands influence the performance of mapping felling events?
- How effectively can Random Forest algorithm map fells using Sentinel-2 data across forest districts with different species compositions?
- What are the sources of misclassification when the model is applied to unseen forest area?
- Which vegetation indices can be used for fell mapping, considering the most effective Sentinel-2 bands for this activity?

2. Theoretical background

2.1. Remote sensing for forest management

Remote sensing has become a central technology in the scientific field of forestry and is also increasingly used in an operational applications (Fassnacht et al., 2024). It is one of the key data sources to fill existing forest management information gaps, particularly in many developing countries. Information retrieved through remote sensing, especially through space and airborne acquisition methods, can offer a synoptic view over large or inaccessible areas (Calders, et al., 2020). One of the advantages of remote sensing data is its ability to provide up-to-date information with short revisit time. Up-to-date information on the current status of forests is not only needed for monitoring and operational planning purposes, but also forms a basis for future management planning and policy formulation (Minunno, et al., 2025).

Remote sensing technology can identify, detect, discriminate, classify, evaluate and measure several forest parameters using two approaches:

- Qualitative analysis (mapping and classification of forest cover types, disturbances, vegetation health, etc.);
- Quantitative analysis (measures the statistical or estimated forest parameters involving biophysical and biochemical parameters like pigments, tree height, diameter, biomass, carbon, basal area, tree density, etc.) (Pandey & Arellano, 2022).

Within forest ecology and management, variables of these analyses are critical for understanding forest ecosystem functions and processes, as well as classifying forests into specific communities, ecosystems, and biomes. In forestry applications, remote-sensing measurements supports forest inventory management by estimating the number of trees per unit area, basal area and timber value (Lechner, et al., 2020). For forest monitoring, species mapping (Francini et al., 2024), forest cover change (Mikeladze et al., 2020) and other variable detection from remote sensing data is important for understanding ecosystem dynamics and anthropogenic impacts in both the short term and long term. From the day-to-day management perspective, monitoring forest change is critical for determining potential risks such as fire hazard due to fuel loads and overall forest health (Lechner, et al., 2020).

In recent years, satellite-based monitoring with year-on-year attribute depictions or characterization of change, have become increasingly common. A great deal of recent applications in remote sensing of forests are focused on using satellite data (such as from

Landsat or Sentinel-2) to map forest attributes and dynamics in a spatially explicit fashion over large areas at an annual time step. Open access to remotely sensed data has been shown to broaden the use of a given dataset, but also to improve outcomes, and enable programmatic use of imagery. Over the past 20-30 years, there has been a significant increase in the use of remotely sensed data from airborne sensors, satellites, and drones to create pixel-based prediction maps of various forest attributes across a wide range of geographical scales and for multiple purposes (Fassnacht et al., 2024). Multispectral imagery data from satellite platforms can be used to scale local forest resource models to larger, regional extents (Massey et al., 2023). Identifying the optimal spatial resolution and level of spatial aggregation, for example, compartment-based classification for such classification maps can improve the effectiveness of forest classification estimates (Nelson et al., 2009).

However, the operational application of remote sensing for forest management is not without challenges. Persistent cloud cover and seasonal effects can substantially reduce the availability of usable imagery (Molnár & Király, 2024). In addition, the complex phenology of forests, varied species compositions and gradients in structural complexity can produce highly variable spectral responses and mixed pixels, complicating classification tasks. Various topographic situations can effect sun-sensor geometries, adding more uncertainty into multi-temporal analyses (Schiller et al., 2024). Together, these factors increase the difficulty of producing consistent, high-quality products of remote sensing data.

2.2. Sentinel-2 data for forest monitoring

Sentinel-2 is a multispectral satellite mission launched in 2015 as part of the European Copernicus Programme. Sentinel-2 has 13 spectral bands, including 4 in the visible range, 4 in the red-edge/NIR range, 2 in the SWIR range and 3 atmospheric correction bands, with spatial resolutions of 10, 20, and 60 meters (Table 1). It consists of three multispectral satellites (Sentinel-2A, Sentinel-2B and Sentinel-2C), providing complete survey of the earth approximately every five days. Sentinel-2 is mainly used for agricultural applications for instance crop monitoring and management, vegetation and forest monitoring, land cover change monitoring for environmental monitoring, observation of coastal areas and others (Pour et al., 2023). Various studies have explored the use of Sentinel-2 in forest applications, such as mapping different forest parameters, for example, forest species (Francini et al., 2024), monitoring forest disturbances (Schiller et al., 2024, Slagter et al., 2023) and monitoring forest

fires, fire severity assessment (Sobrino et al., 2024). Moreover, Sentinel-2 data has been extensively used for analyzing forest canopy structure, including canopy closure which are essential for assessing forest health and productivity (Mikeladze et al., 2020).

Table. 1. Sentinel-2 spectral bands and characteristics (Pelc-Mieczkowska, 2021).

Sentinel-2 band	**Central wavelength (nm)**	**Resolution (m)**
Band 1 (Coastal aerosol)	443	60
Band 2 (Blue)	490	10
Band 3 (Green)	560	10
Band 4 (Red)	665	10
Band 5 (Vegetation Red-edge 1)	705	20
Band 6 (Vegetation Red-edge 2)	740	20
Band 7 (Vegetation Red-edge)	783	20
Band 8 (Near-InfraRed)	842	10
Band 8A (Near-InfraRed narrow)	865	20
Band 9 (Water vapour)	945	60
Band 10 (Cirrus detection)	1375	60
Band 11 (SWIR 1)	1610	20
Band 12 (SWIR 2)	2190	20

The importance of specific Sentinel-2 bands typically depends on the application, as different bands provide unique information relevant to various monitoring objectives. A study on tree species classification identified the SWIR (band 11 and band 12), red-edge 1 (band 5), and two visible bands (band 2 and band 4) as the most important. Similarly, band 2, band 5 and band 11 were also found to be important in crop classification (Immitzer et al., 2016). Additionally, red-edge bands (band 5, band 6, band 7) in Sentinel-2 may offer more accurate and effective land cover classification capabilities in boreal landscapes compared to conventional vegetation indices (Abdi, 2019). In terms of felling detection, several Sentinel-2 spectral bands have shown strong potential for detecting forest felling due to their sensitivity to changes in vegetation structure and health. Band 12 (SWIR 2) is particularly responsive to moisture content and canopy structure, making it useful for identifying disturbances caused by tree removal. Notable shifts in its reflectance values often indicate recent felling activity. Similarly,

bands 4 (red) and 8 (NIR) are highly effective in detecting vegetation loss, as felling typically results in a marked decrease in NIR reflectance due to the removal of healthy vegetation. Band 3 (green), which reflects strongly from healthy vegetation, also contributes to overall forest monitoring. Additionally, previous studies have emphasized the value of bands 3, 8, and 12 in modeling canopy closure (Mikeladze et al., 2020), a key indicator for felling detection, as tree harvesting significantly impacts canopy density and openness.

2.3. Forest felling practices in Latvia

Latvia's forestry sector employs a variety of felling methods, each serving specific forest management objectives. The main types of forest felling include:

- Thinning

Thinning is carried out during the forest stand development cycle to change the species composition and improve growth conditions for the remaining trees. It begins with pre-commercial thinning in young stands, especially when fast-growing species begin to outcompete target species. Thinning ensures an optimal species mix and provides adequate growing space for selected trees, promoting healthier and more productive forests.

- Main felling

Main felling is applied once a stand reaches the maturity age or diameter thresholds defined by forest law. One method of main felling is clear-cutting, where the entire stand is harvested in a single operation. By law, areas after clear-cutting must be regenerated through planting, seeding, or natural regeneration. The maximum allowable area for a clear-cut depends on the forest type and is limited to 2 or 5 hectares.

- Sanitary felling

This type of felling targets trees that have lost their vitality due to wind, snow, fire damage, pests, or disease. Even if the stand has not yet reached final felling criteria, sanitary felling is used to remove dead or weakened trees, helping to prevent the spread of damage and maintain forest health.

- Reconstructive felling

Reconstructive felling is carried out in unproductive stands, as defined by regulations. This includes stands with basal areas below critical thresholds or young stands (under 6 meters in height) where over 60% of trees are damaged by animals, pests, or diseases. It also applies to mature pine, spruce, or birch stands over 40 years old—or pine stands over 70 years old—where more than 40% of the growing stock consists of low-value species such as aspen, grey alder, or willow.

- Landscape felling

Landscape felling is used to improve scenic views by revealing landscape features, cultural heritage sites, or natural landmarks. This type of felling can only be performed if included in a forest management plan, a nature protection plan for specially protected areas, or approved by a landscape architect (Rozentāls, et al., 2017).

In 2023, over 165 thousand hectares of forest were felled in Latvia. The largest areas were affected by main felling (>58 000 ha), thinning (>49 000 ha), and sanitary felling (>47 000 ha) (Figure 1). In terms of felled volume, main felling accounted for the largest share, with 14.2 million m^3, followed by sanitary felling, with 2.6 million m^3 (Figure 2). This highlights the characteristics of each felling type: although the felled areas for main, thinning, and sanitary felling are relatively similar, the volumes of harvested wood differ significantly.

Different felling types can be challenging to detect using remote sensing data. For example, main fellings may also be performed in stages, known as shelterwood felling, or selectively, known as selective cutting, where only part of the stand is harvested periodically (Rozentāls, et al., 2017). In compartment-based classification it can create totally different reflectance values in the same compartment. Furthermore, because varying degrees of canopy removal occur across all felling types, the resulting spectral responses may be similar, leading to overlap in reflectance changes between different felling types.

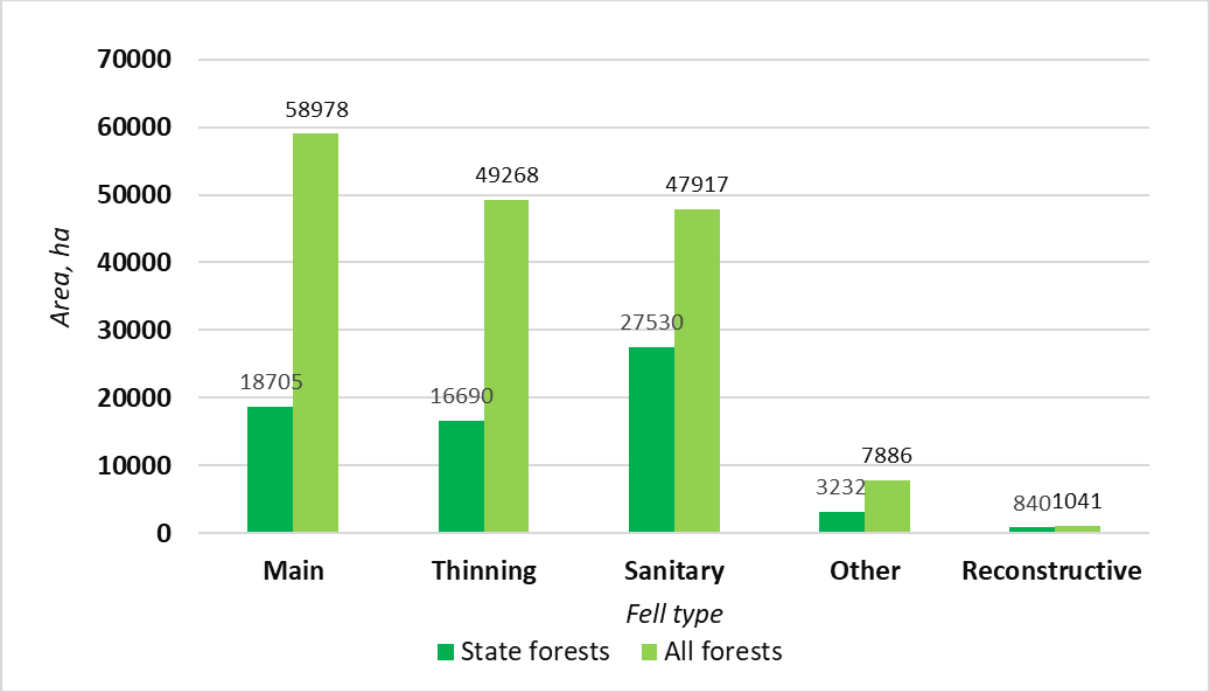

Figure 1. Felling area indicated in tree felling license by type of felling, year 2023 (Central Statistical Bureau of Latvia, 2024).

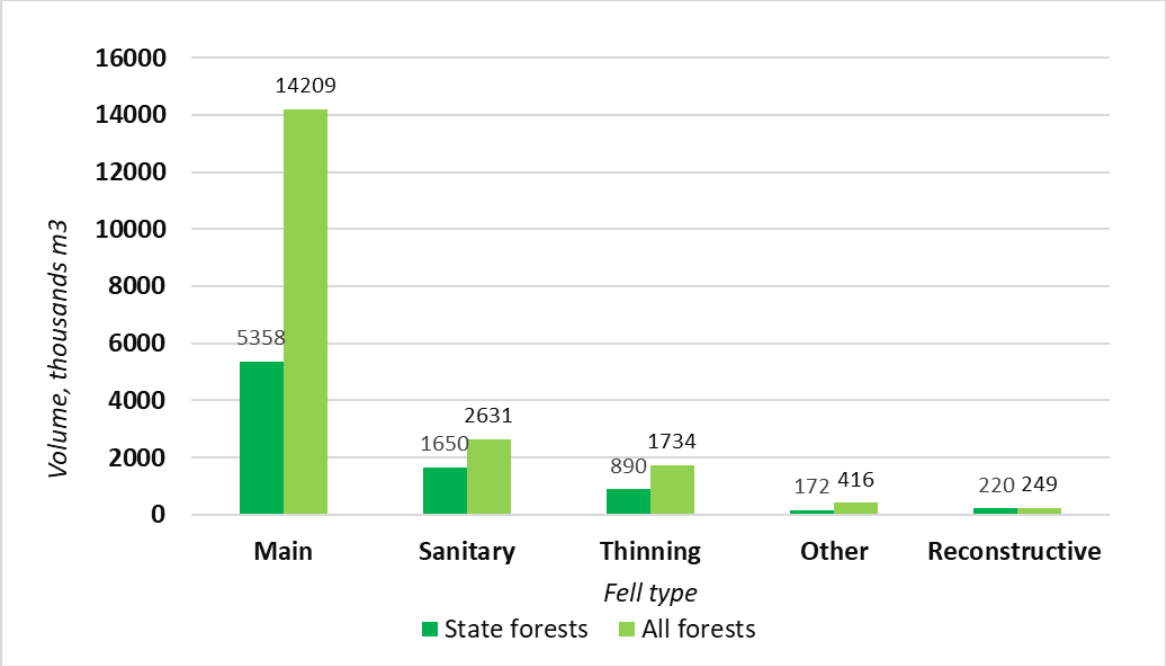

Figure 2. Felling stock volume indicated in tree felling license by type of felling, year 2023 (Central Statistical Bureau of Latvia, 2024).

2.4. Machine learning techniques in remote sensing-based forest analysis

Machine learning (ML) is a subdivision of AI in which the machine learns from machine-readable data and information. It uses data, learns the pattern and predicts the new outcomes. Its popularity is growing because it helps to understand the trend and provides a solution that can be either a model or a product (Upreti, 2022). There are four types of ML approaches (Table 2):

Table. 2. Machine learning algorithm types (SAS, 2025).

Machine learning algorithm type	**Description**	**Examples of algorithms**
Supervised	Predicts a class/category, based on a given set of features, using probability.	Random Forest, Support Vector Machine, Decision Trees, k-Nearest Neighbor.
Unsupervised	Categorize unlabeled data, i.e. data without defined categories or groups.	K-means, Principal Component Analysis (PCA).
Semi-supervised	Uses both supervised and unsupervised learning.	Graph-based methods, self - training, neural networks.
Reinforcement learning	Focuses on regimented learning processes, where a machine learning algorithm is provided with a set of actions, parameters and end values.	Q-learning, Deep Q Networks.

Among the different ML approaches, supervised learning is especially effective for satellite image classification tasks. Within this category, the RF algorithm stands out as one of the most commonly applied techniques in remote sensing. The popularity of this algorithm is due to the fact that it can be used for both classification and regression purposes, and thus can be used with categorical and continuous variables (Abdi, 2019). It has been the most popular machine algorithm to link remote sensing data to forest structural attributes, such as forest aboveground biomass, canopy cover, forest fire susceptibility (Calders, et al., 2020) or doing forest species classification tasks and object-oriented mapping (Abdi, 2019).

Compared to other machine learning classifiers, the RF algorithm demonstrates notable strengths for remote sensing tasks:

- Studies have shown that Support Vector Machine, RF, and k-Nearest Neighbor classifiers can achieve similarly high overall accuracies. However, RF tends to be preferable when training data are balanced or when larger sample sizes are available (Noi & Kappas, 2017);
- RF performs well with high-dimensional input data, while other classifiers often struggle with dimensionality and highly correlated variables (Belgiu & Drăguţ, 2016);
- RF is a robust classifier even under low levels of class label noise, thanks to its bootstrap sampling and random feature selection during tree construction (Pelletier et al., 2017). It does not need temporal preprocessing like neural networks, as it can directly classify per-pixel data without temporal dependence (Belgiu & Drăguţ, 2016);
- Compared to deep learning approaches, RF has the advantage of requiring less labeled training data. Deep learning models often risk overfitting and poor generalization when labeled data are limited. While deep learning is widely used for natural image classification, remote sensing data are more complex due to the variety of sensors involved. Deep learning requires designing network architectures specifically suited for remote sensing image classification (Yang et al., 2018), while RF can be applied directly with minimal parameter tuning (Pelletier et al., 2017).

2.5. Vegetation indices used for forest monitoring and classification

Vegetation indices are mathematical combinations of spectral bands designed to identify the state of vegetation. Their values are obtained from appropriate combinations of reflectance measured in individual spectral bands (Pelc-Mieczkowska, 2021). To track vegetation state in satellite images, different types of indices can be used (Manjunath et al., 2014):

- Structural indices

Structural indices primarily capture information about canopy structure and vegetation density.

Table 3. Examples of structure-oriented vegetation indices.

Index	Formula (Sentinel-2)	Description
Normalized Difference Vegetation Index (NDVI)	(B08-B04)/(B08+B04)	Estimates the photosynthetic activity by a combination of Red and Near Infrared bands that are generally conditioned by the presence of chlorophyll (Spadoni et al., 2020).
Soil Adjusted Vegetation Index (SAVI)	1.5*((B08-B04)/(B08+B04+0.5))	Derived from NDVI, SAVI index is focused on minimizing impact of soil optical properties on vegetation reflectance (Huete, 1988).
Enhanced Vegetation Index (EVI2)	2.5*((B08-B04)/(B08+2.4 *B04+1))	Developed to optimize the vegetation signal with improved sensitivity in high biomass regions. This version of index removes blue band from the original EVI formula to simplify calculation (Zhangyan et al., 2008).

- Chlorophyl/pigment indices

Pigmentation-oriented indices primarily measure chlorophyll content and photosynthetic activity (Table 4).

Table 4. Examples of pigment-oriented vegetation indices.

Index	Formula (Sentinel-2)	Description
Structure Intensive Pigment Index (SIPI)	(B08-B01)/(B08-B04)	Designed to assess carotenoid to chlorophyll ratio from leaf spectral reflectance while minimizing effects of the surface and leaf internal mesophyll structure (Penuelas et al., 1995).
Visible Atmospherically	(B03-B04)/(B03+B04-B02)	Calculated using only visible spectrum bands designed to reduce atmospheric

Resistant Index (VARI)		effects and enhance sensitivity to vegetation cover (Gitelson et al., 2002).
Red Edge Chlorophyll Index (RECI)	(B08/B06)-1	Estimates the chlorophyll content of leaves by utilizing the high sensitivity of the red-edge spectral region to chlorophyll concentration (Clevers & Gitelson, 2013).

- Water sensitive indices

Water sensitive indices detects changes in water content or moisture in plants or soil (Table 5).

Table 5. Examples of water sensitive vegetation indices.

Index	**Formula (Sentinel-2)**	**Description**
Normalized Difference Moisture Index (NDMI)	(B08-B11)/(B08+B11)	Used to assess vegetation liquid water content using near-infrared and shortwave infrared reflectance, offering reduced atmospheric sensitivity and vegetation water status information complementary to NDVI (Gao, 1996).
Moisture Stress Index (MSI)	B11/B08	Calculated as the ratio of a SWIR to a NIR band, which can detect changes in leaf water content (Hunt & Rock, 1989).
Normalized Difference Water Index (NDWI)	(B03-B08)/(B03+B08)	Uses green and near-infrared bands to highlight differences in water content of water bodies (Gao, 1996).

3. Methods and material

3.1. Study areas

Study areas for this research were selected in Latvia, a country where forestry holds a central role in economy with forests covering more than a half of the national territory. Latvian forestry companies, particularly the Latvian State Forests (LSF) have shown growing interest in leveraging remote sensing data and analysis for operational planning and forest change detection. Studies performing these methods for Latvian forest management are still limited, and such data are essential to make forest monitoring faster, cheaper, more precise and scalable.

As part of the research, the selection of the study areas under investigation played an important role. To ensure comprehensive geographic coverage and meaningful analysis, forest districts were chosen based on geographic diversity across Latvia and the number of clear-cut felling conducted between 2019 and 2024 (Figure 3).

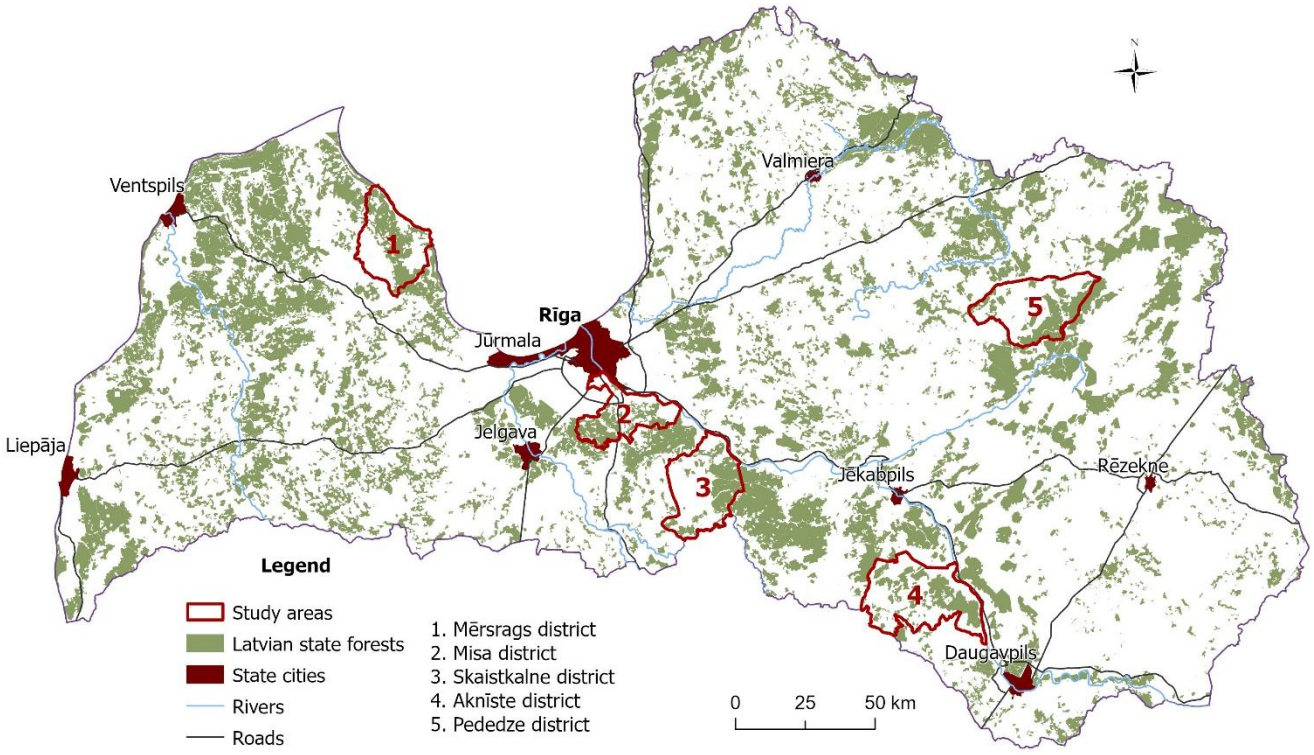

Figure 3. Locations of study areas (Produced by author using LVM GEO, 2025 and Envirotech, 2021 data).

The study areas are districts within the LSF that rank among the highest in terms of felling activity:

- Mērsrags District – Located in the western part of Latvia, the district covers 62 235 ha and comprises 17 931 forest compartments. The district recorded the highest number of clear-cuts (1221) between years 2019 and 2024. It lies along the coast of the Gulf of Riga and is the closest district to the Baltic Sea, with forests predominantly composed of pine (52 % of forest compartments have pine as main species) adapted to coastal and sandy soils. Additional species like birch covers 22 % and spruce 19 % of total district compartments.
- Misa District – Located in the central part of the country, district covers 46 082 ha with 11 770 forest compartments and ranks eighth with 1011 clear-cuts. The district is characterized by a mixed-use landscape, combining productive agricultural land and managed forests, moderate continental climate and fertile soils. Dominant tree species are pine (55 %). Spruce, birch and black alder each cover more than 10 % of district compartments.
- Skaistkalne District – Located in central/southern Latvia, district covers 69 857 ha with 17 221 forest compartments and ranks fourth with 1049 clear-cuts. District is known for flat terrain and fertile soils, includes parts of large forest massifs of Sēlija region. Dominant tree species are pine (56 %), birch (20%) and spruce (14 %).
- Aknīste District – Representing the southern region of Latvia, it is the largest of selected districts with area 86 357 ha and 15 606 forest compartments. District ranks second in clear-cuts (1078). The area has a more continental climate, varied terrain and diverse forest types like mix of coniferous and broadleaf species. In this district pine compartments covers only 22 % of total district area. 29 % covers birch, 22 % spruce and 8 % aspen compartments
- Pededze District – Located in the eastern Vidzeme Upland, district covers 71 695 ha with 15 499 forest compartments and recorded the twelfth highest number of clear-cuts (969). District is known for its cooler climate, hilly terrain and extensive forest cover. Dominant tree species are birch (30 %), pine (29 %) and spruce (23 %).

Fellings of Mērsrags, Aknīste, Misa and Pededze districts were used in model training and self-model testing. The Skaistkalne district served as independent evaluation area – a forest district that was not included in the training dataset - therefore not seen by the RF model during

training, and thereby providing information on the transferability of the model. This district was used for model performance statistical measurement assessment.

3.2. Data

- Sentinel-2 data

Sentinel-2 Level-2A surface reflectance imagery was used to extract spectral information for the analysis (Table 6). Sentinel-2 scenes for the years 2018 (image before felling activity) and 2024 (image after felling activity) were queried and filtered by spatial extent (based on predefined district polygons) and temporal range (May to September) using the Earth Search STAC API. Only scenes with cloud cover less than 5% were used to ensure high data quality. Multiple partially overlapping scenes were mosaicked to provide seamless coverage when no single scene could completely cover the area of interest. The Scene Classification Layer (SCL), which was used to mask low-quality pixels like clouds and shadows, were used along with spectral bands to ensure only clear-sky observations are used for image analysis. Bilinear interpolation was used to resample all bands to a resolution of 10 meters. Bands 1, 9 and 10 were excluded from analysis as they are not typically used for surface reflectance analysis.

Table. 6. Sentinel-2 imagery acquisition details by forest district.

Forest district	Year	Acquisition date	Cloud cover, %
Mērsrags	2018	2018-08-23	0.0422
	2024	2024-05-21	0.0009
Misa	2018	2018-08-01	0.0005
	2024	2024-05-21	0.3677
Skaistkalne	2018	2018-05-12	0.0107
	2024	2024-06-27	0.2361
Aknīste	2018	2018-08-23	0.0082
	2024	2024-06-27	0.1955
Pededze	2018	2018-05-12	0.0056
	2024	2024-06-27	0.1011

- Data of Latvian State Forests

Data on fellings of Latvian State Forests were primary information source for the analysis. Data was acquired in GDB format (Geodatabase file format used in ESRI GIS software) and filtered out to include only completed felling operations performed between 2019 and 2024, while excluding felling that occurred after the acquisition date of the 2024 Sentinel-2 imagery. In this research, only fells classified as main fellings were analyzed as this type is best suited for Sentinel-2 reflectance analysis, because most of the forest trees are cut. In practice, these fellings correspond to clear-cuts, with over 99 % of selected main fellings involve harvesting the entire stand.

To acquire forest district data, Latvian State Forests open-source spatial data in SHP format were used (LVM GEO, 2025). Also, open-source forest compartment data were used to provide non-felled data to training and test data to fells modelling. Forest compartments, which were not intersected by clear-cut felling polygons were labeled as non-fells class. When combined non-fells and fells datasets into RF classifier, algorithm learned the spectral and structural differences between felled and unfelled compartments. Data on dominant tree species for each compartment were used to evaluate the performance of RF model.

3.3. Methods description

All data processing, modelling and analysis were implemented using the Python programming language to avoid manual work, to ensure reproducibility and to enable analysis for geographic areas outside of training dataset. Geospatial libraries like *arcpy* and *geopandas* were used in spatial data processing and model assessment in the evaluation area. RF modelling and evaluation metric analysis were performed by *sklearn* library. Additional libraries like *pystac_client* for Sentinel-2 data download and *matplotlib* were used for visual representation of results. The ArcGIS Pro environment was used for spatial data visualization tasks.

- Spatial data processing

Model training data were compiled from clear-cut felling events recorded between 2019 and 2024 and rest of study areas forest compartments where no felling took place. Training data were used to create a RF classification model, which aims to identify areas affected by clear-cut forest felling based on changes of spectral signatures in Sentinel-2 imagery.

Sentinel-2 imagery were obtained for two periods: a reference year before the clear-cut activity (2018) and after clear-cut period (after May of 2024). The raster datasets were processed by individual Sentinel-2 band and clipped to study areas. If multiple imageries were overlapping in study areas, image with less cloud cover were used. Raster datasets of reflectance difference were created based on formula:

*diff_raster = ((band_reflectance_2024 – band_reflectance_2018) / band_reflectance_2018 * 100)*

These raster datasets represented percentage change in reflectance for each Sentinel-2 band (Figure 4).

Using ArcGIS geoprocessing tool *Zonal Statistics as Table*, median values of reflectance difference were calculated for each Sentinel-2 band. According to SCL Sentinel-2 pixels, which were affected by clouds, were not used in analysis. The median method was used to reduce the effects of extreme reflectance values from pixels near clouds that were not masked using SCL layer. The resulting layer of each study area was represented as a forest compartment layer, which contained the median percentage differences in reflectance values of Sentinel-2 bands from before and after felling. A label field was added, in which the value of 1 indicated the presence of clear-cut activity, while 0 indicated no clear-cut activity.

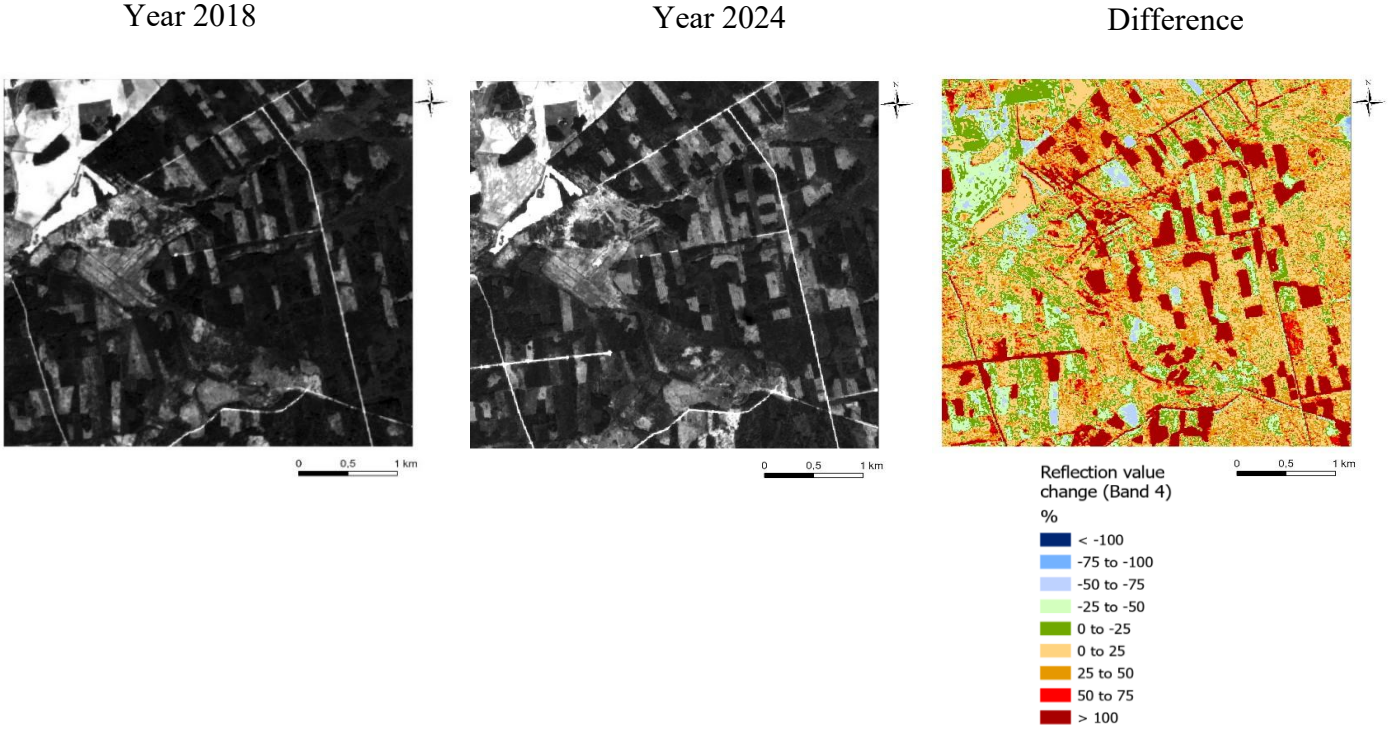

Figure 4. Red visible band (band 4) reflectance change (%) based on Sentinel-2 Imagery from 2018 to 2024.

- Random forest classification

The RF algorithm was used to determine the significance of different Sentinel-2 spectral bands in detecting felling activities across different Sentinel-2 images. The classifier was trained using 80/20 train-test split as this proportion represents the average used in similar analysis, typically between 70/30 and 90/10 (Immitzer et al., 2016, Mohammadpour et al., 2022). As input data had imbalance between fells and non-fells (forest compartments), class weights were applied based on the ratio of clear-cut and non-felled forest compartment count. Input data consisted of forest compartments of Mērsrags, Aknīste, Misa and Pededze districts and were evaluated on the testing subset, which was randomly selected from the overall dataset. The RF model dataset included a total of 4 046 fells and 41 056 compartments. With a felling ratio of 1:9, class weights were applied to address class imbalance. By giving class weights, it is ensured that the model gives appropriate attention to minority classes (fells). The metrics included accuracy of positive predictions (precision), a confusion matrix and a classification report with different parameters (Table 7). Permutation-based feature importance was applied using the implementation available in the scikit-learn library. This method estimates the importance of each predictor variable by randomly permuting its values and measuring the resulting decrease in model performance. In this study, permutation importance was calculated on the independent test subset (20% of the data) rather than on the training data. This ensures that feature importance reflects the model's generalization performance rather than its ability to fit the training data. Feature importance analysis was used to evaluate how much the model relies on such particular feature, in this case Sentinel-2 band. The resulting importance scores reflect which spectral bands affected the model's accuracy, and helped to inform which bands are the most important in such a classification task.

Table 7. Description of Random Forest classification report metrics.
(ESRI, 2025; SOCR, 2025; Scikit-learn developers, 2025).

Parameter name	Description
User accuracy (Precision)	Measures errors of commission, where pixels are misclassified as a known class when they should have been classified as different class, Values ranges from 0 (worst) to 1 (best).
Producer accuracy (Recall)	Measures false negatives, indicating how well the classification results align with expectations of the creator. Values ranges from 0 (worst) to 1 (best).

Overall accuracy	Probability that a sample will be correctly classified. The best value is 1 and the worst value is 0.
F1 score	Harmonic mean of the precision and recall, where an F1 score reaches its best value at 1 and worst score at 0. The relative contribution of precision and recall to the F1 score are equal.
Feature Importance	Measures the contribution of each feature to a fitted model's statistical performance on a given tabular dataset. Larger value indicates that feature has greater importance for the model. Used to measure Sentinel-2 band importance.

- Model evaluation

The RF model testing consisted of two procedures: the first included self-testing on Sentinel-2 band median difference values extracted from four study areas used in the model training. Prior to model training, the dataset was randomly split into training (80%) and testing (20%) subsets, having 35 786 training samples and 8 947 independent testing samples. The partitioning was performed using a fixed random seed value of 42 to ensure reproducibility of the results. The value of the seed does not influence the methodological validity, but ensures that identical training and testing subsets can be recreated.

The second testing phase included model testing on separate study area (Skaistkalne district) unseen by model. This dataset included 958 fells and 16 689 compartments. The classification was evaluated by comparing which compartments are classified as fells against ground-truth labels (performed fells). Evaluation metrics were calculated using the following four quantities:

- True positive (TP) - Predicted fell matches actual fell
- False positive (FP) - Predicted fell where fell has not occurred
- False negative (FN) - Missed actual fell
- True negative (TN) - Correctly predicted non-fell compartment

Using these quantities different accuracy metrics were calculated:

- Overall accuracy: $OA = (TP + TN) / (TP + TN + FP + FN)$
- Producer accuracy: $PA = TP / (TP + FN)$
- User accuracy: $UA = TP / (TP + FP)$
- F1 score = $(2 * UA * PA) / (UA + PA)$

- Vegetation indices analysis

To evaluate the effect of vegetation indices on classification performance, a limited set of the three indices were added to band modelling process. The indices were selected to represent different types of vegetation index categories, incorporate the most influential spectral bands and index relevance for clear-cut forest detection:

  - NDVI (Normalized Difference Vegetation Index) - represents the structural index category, selected as it is one of the most widely used indices in remote sensing research.
  - VARI (Visible Atmospherically Resistant Index) – represents the chlorophyll/pigment index category, selected as it uses visible bands, which were identified as the one of the most important bands in analysis.
  - NDMI (Normalized Difference Moisture Index) – represents the water-sensitive index category, most suitable water-sensitive index for forest felling as it effectively captures changes in canopy moisture.

4. Results

4.1. Band Importance

The results highlighted five spectral bands of Sentinel-2 with high importance scores: band 4 (red), band 12 (SWIR2), band 11 (SWIR1), band 3 (green) and band 2 (blue) showed clear importance gap compared to the other bands (Figure 5).

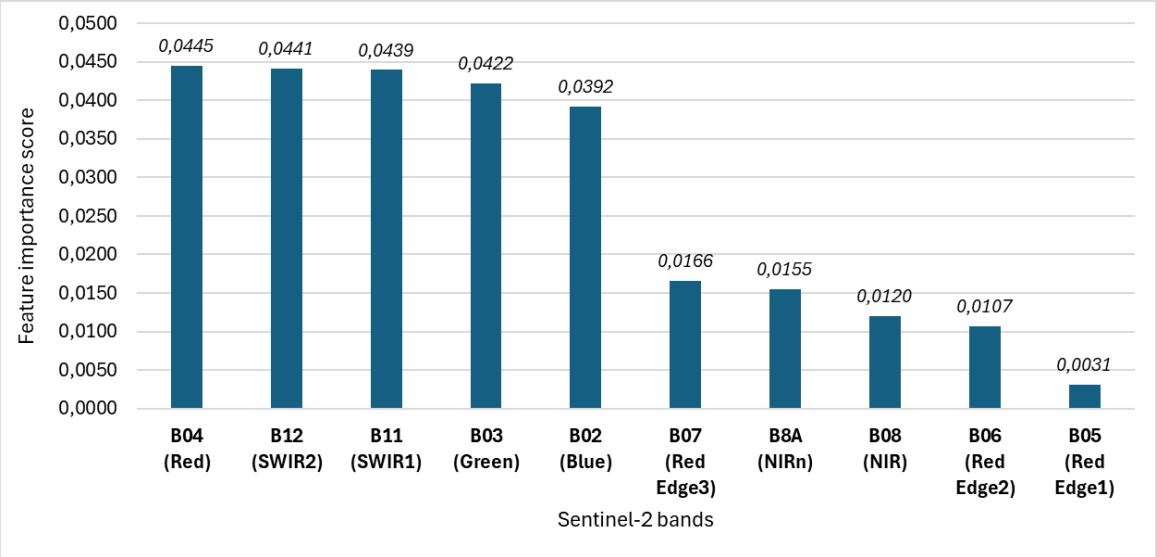

Figure 5. Sentinel-2 band importance scores for forest felling detection.

The RF model assigned the highest importance scores to the red and SWIR bands, indicating that these bands contributed most strongly for detecting forest felling. Red edge bands (band 5, band 6, band 7) and NIR (Band 8, Band 8A) showed notably lower importance. For each forest compartment, median reflectance values were derived before and after felling event. The relative percentage change was then calculated per compartment using the pre-felling reflectance as the reference, and the resulting percentages were averaged across all compartments. Bands 2, 4, 11, 12 showed relative increases greater than 100% (Figure 6).

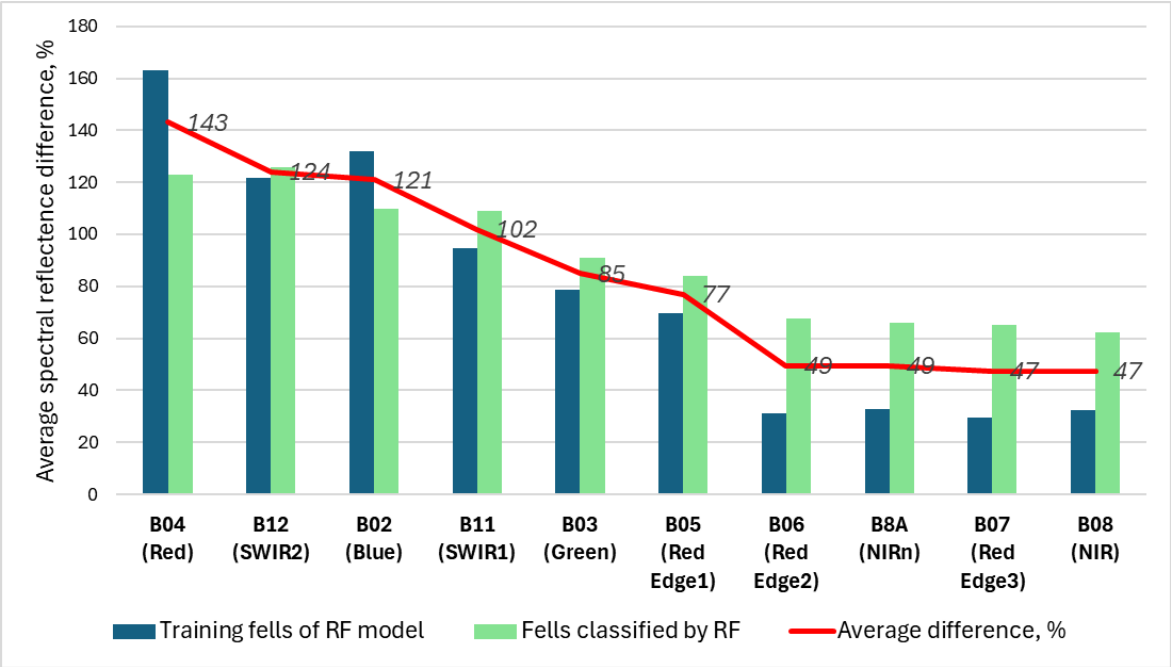

Figure 6. Sentinel-2 band average spectral reflectance change (%) due to forest felling.

4.2. Performance of the Random Forest model

Although results achieved high overall accuracy and showed similar results on both testing methods (0.96 for self-testing and 0.97 for unseen area testing), this metric was influenced by class imbalance. Greater emphasis was placed on the F1 score, which balances the precision (user's accuracy) and recall (producer's accuracy). The F1 score decreased from 0.78 in self-testing to 0.73 in unseen-area testing, indicating classification errors when applied model to new, unseen data. Similar differences were found in users and producer's accuracy. However, relatively small differences between testing methods suggest stable and transferable performance in detecting felling events (Table 8).

Table 8. Random Forest model classification accuracy metrics.

	Results of model self-testing	Results of model unseen area testing
Overall accuracy	0.96	0.97
User's accuracy	0.80	0.74
Producer's accuracy	0.76	0.73
F1 score	0.78	0.73

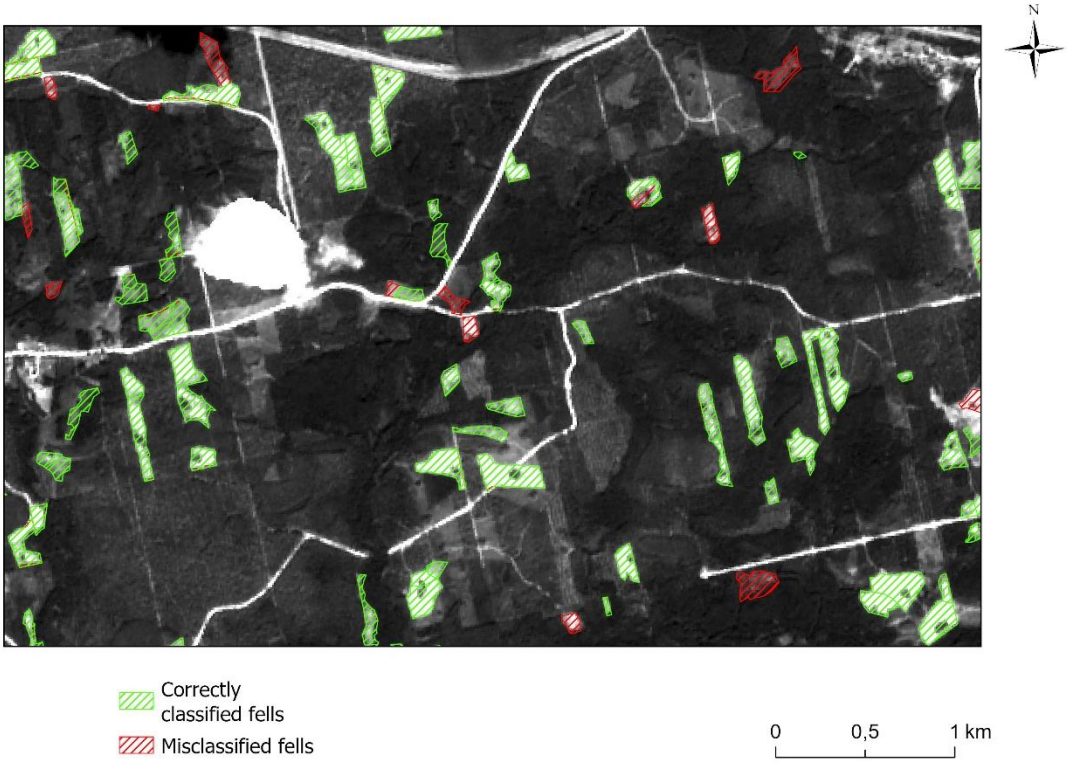

Figure 7. Area of well-performing fell classification in Skaistkalne district.

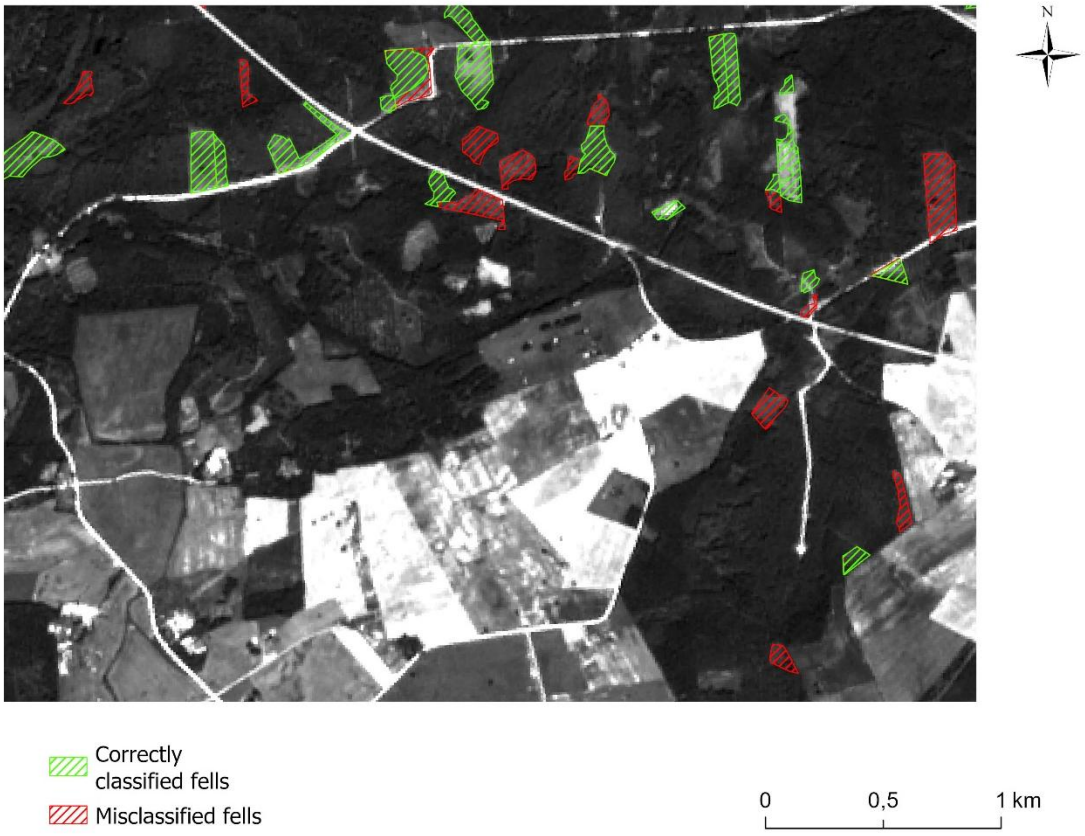

Figure 8. Area of low classification accuracy in Skaistkalne district.

4.3. Classification patterns and sources of misclassification

An analysis of median spectral difference values across classification outcomes was conducted to examine the spectral characteristics associated with different prediction results (Figure 9). The results showed clear spectral differences between non-felled compartments and fells. The spectral differences between 2018 and 2024 in non-felled compartments remain relatively low, around 20 reflectance units, reflecting their stable canopy conditions. Missed fellings (FN) showed lower reflectance differences in the visible and SWIR bands (30-60 reflectance units), which led the model to classify them as non-felled areas. In contrast, overestimated fellings (FP) exhibit higher reflectance differences (90-130 reflectance units) in the visible (bands 2, 4) and SWIR bands, which were one of the most important bands in the RF model. Correctly classified fellings (TP) exhibit intermediate spectral difference values between missed (FN) and overestimated (FP) cases. In the band 4 (red), TP values range approximately from 80–100 units, compared to 30–60 units for FN and 100–120 units for FP. A similar pattern is observed in the SWIR bands, where TP values (100–110 units) lie between those of FN (50–60 units) and FP (120–140 units), indicating these bands as most important for distinguishing clear-cut fells.

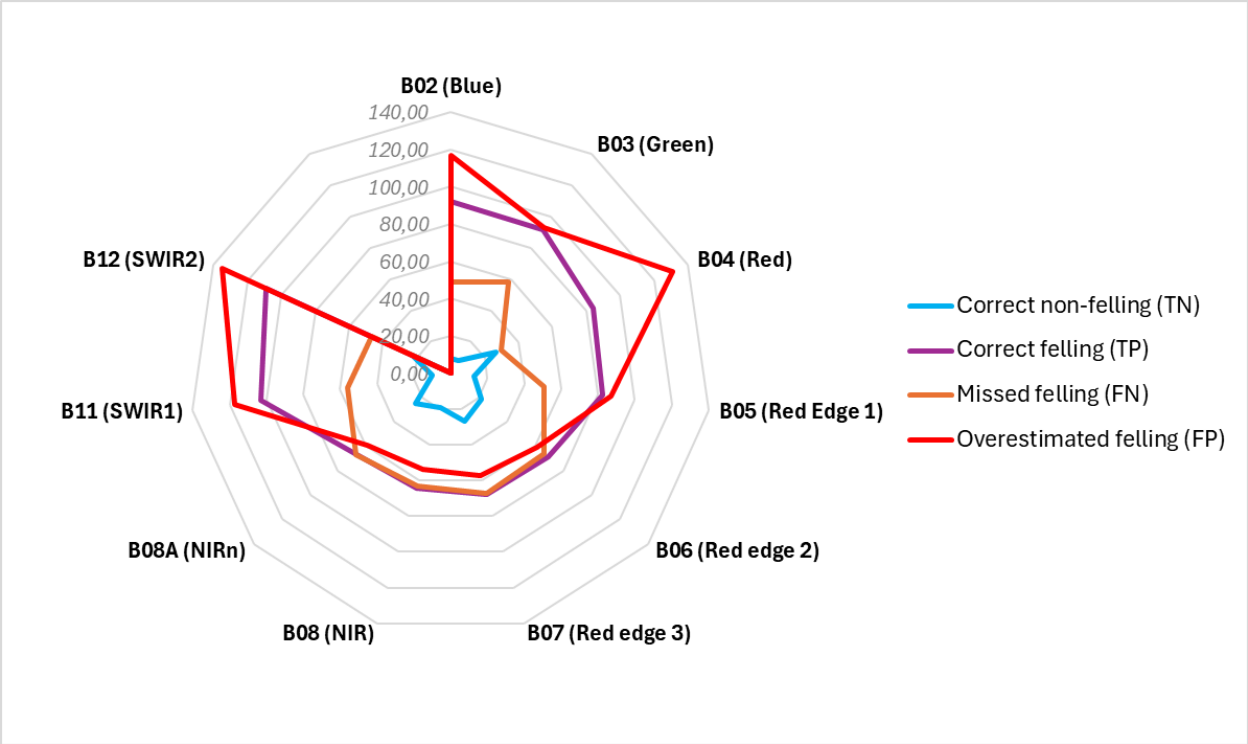

Figure 9. Median spectral difference (2018-2024) by classification outcome.

To better understand how the RF model performs across different forest compartments, classification results were divided into three equal groups based on compartment size using equal-frequency stratification. The groups of compartments were defined as small (< 0.72 ha), medium (0.72-1.41 ha) and large (>1.41 ha) and this stratification enabled assessment of whether spatial extent influences classification accuracy. Each group consisted of 5563 forest compartments. The distribution of classification outcomes (TP, TN, FN, FP) was examined across the different compartment size groups.

The results showed that large compartments group generally achieved higher proportion of correctly classified fells (TP) and non-fells (TN), but small compartments were more prone to the misclassification (Figure 10). More than 50% of overestimated fellings were identified within the small compartments. Also, small compartments accounted for just over 20% of the total correctly classified fells, while the large compartments contributed roughly twice this amount. These findings suggest that compartment size affects the reliability of classification, with the model performing better in larger compartments.

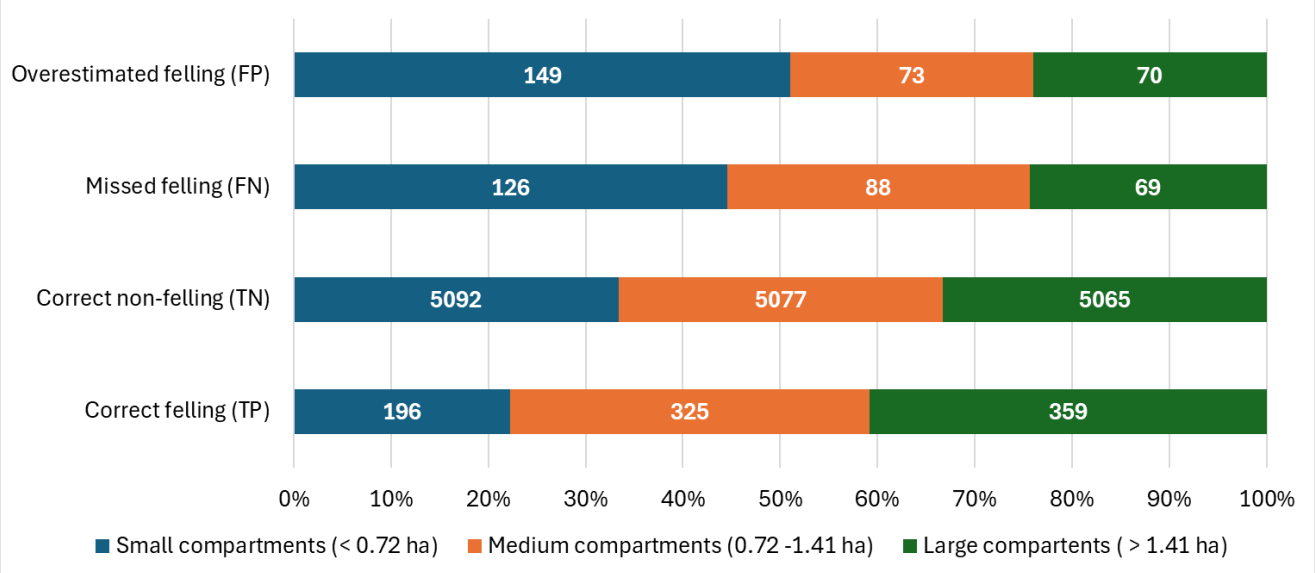

Figure 10. Distribution of fell classification accuracy by forest compartment size.

To examine classification patterns based on tree species level, the RF model was evaluated against forest compartment dominant species (Table 9). The model performed well for pine, birch and aspen, but struggled with spruce and gray alder dominant species compartments. In spruce dominated compartments, the model often overestimates clear-cut felling events, producing high number of false positives.

Table 9. Random Forest classification by dominant tree species in forest compartments.

Species	**Correct non-felling (TN)**	**Correct felling (TP)**	**Missed felling (FN)**	**Overestimated felling (FP)**	**User accuracy**	**Producer's accuracy**	**F1 score**
Pine	7224	529	118	86	0.86	0.82	0.84
Spruce	2573	88	30	189	0.32	0.75	0.45
Birch	3429	210	83	12	0.95	0.72	0.82
Black Alder	1295	30	36	3	0.91	0.45	0.61
Aspen	160	21	9	0	1	0.70	0.82
Gray Alder	*50*	*2*	*7*	*0*	*1*	*0.22*	*0.36*

During evaluation of the RF model, several sources of misclassification were identified that affected fells detection. Pixels of Sentinel-2 image were affected by clouds – some pixels near clouds were not fully masked by SCL. These pixels have extreme reflectance values, which caused the model to incorrectly classify nearby forest compartments as fellings (Figure 11). The SCL cloud masking was insufficient to fully remove cloud affected pixels, due to the absence of additional buffering around cloud boundaries.

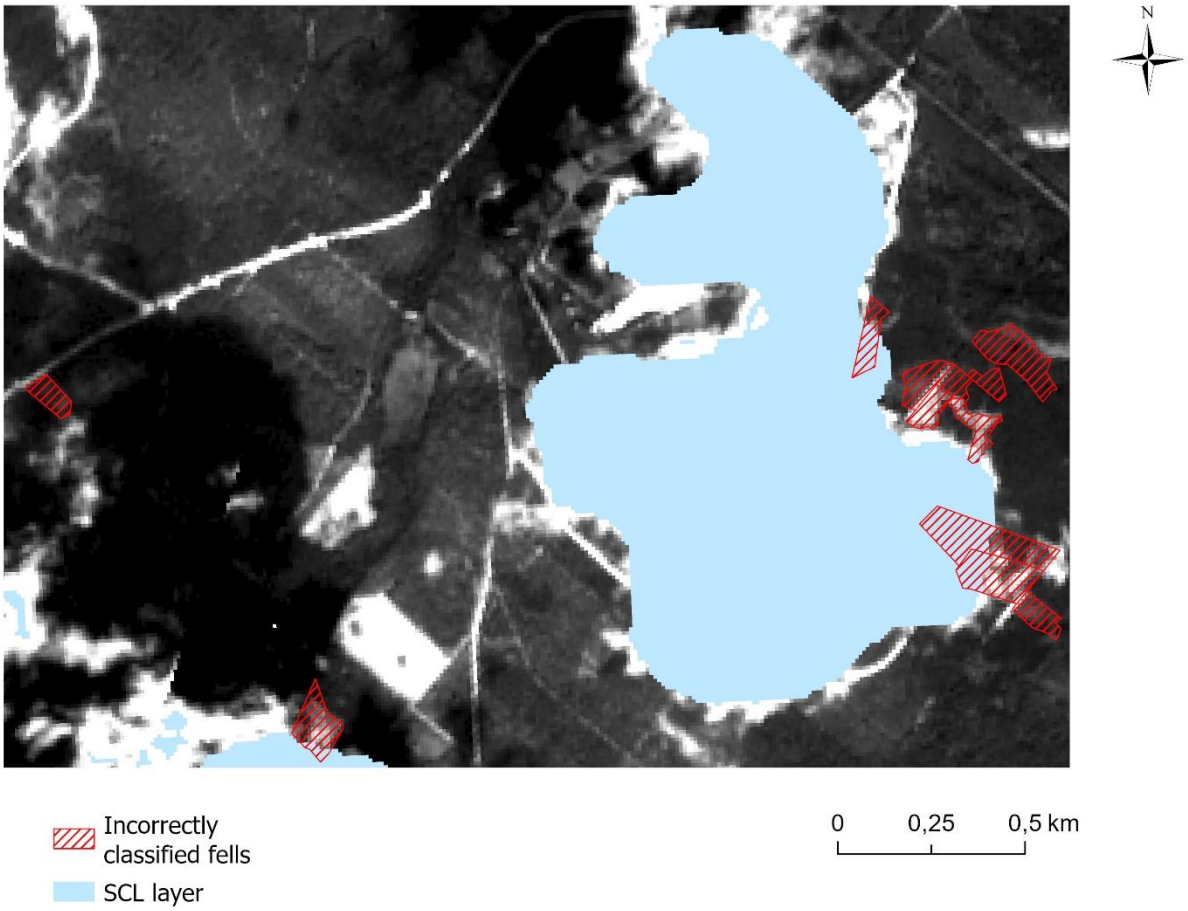

Figure 11. Overestimated fellings near clouds – Skaistkalne district.

The model was trained and validated on clear-cut felling events, but forest compartments may experience other felling types. The results showed that the model often overestimates clear-cut felling where other felling types occurred (Figure 12). This was particularly evident for sanitary felling, the most common non-clear-cut type, where compartments were frequently misclassified (Figure 13).

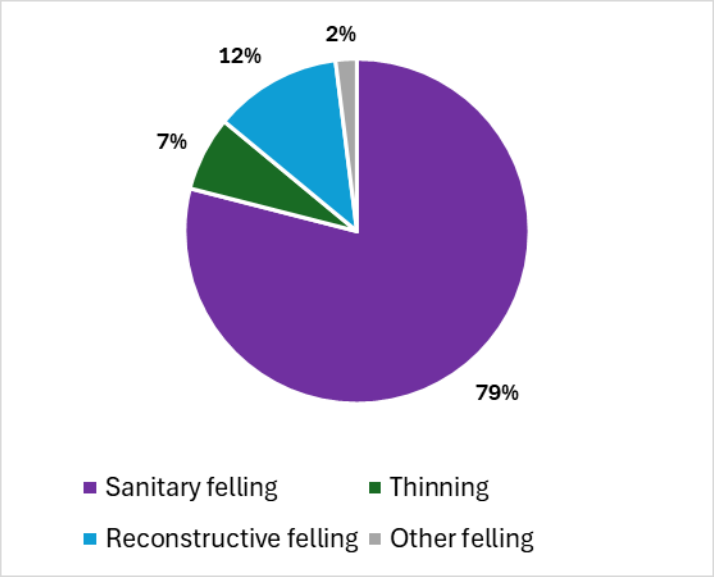

Figure 12. Random Forest model overclassification distribution by felling type.

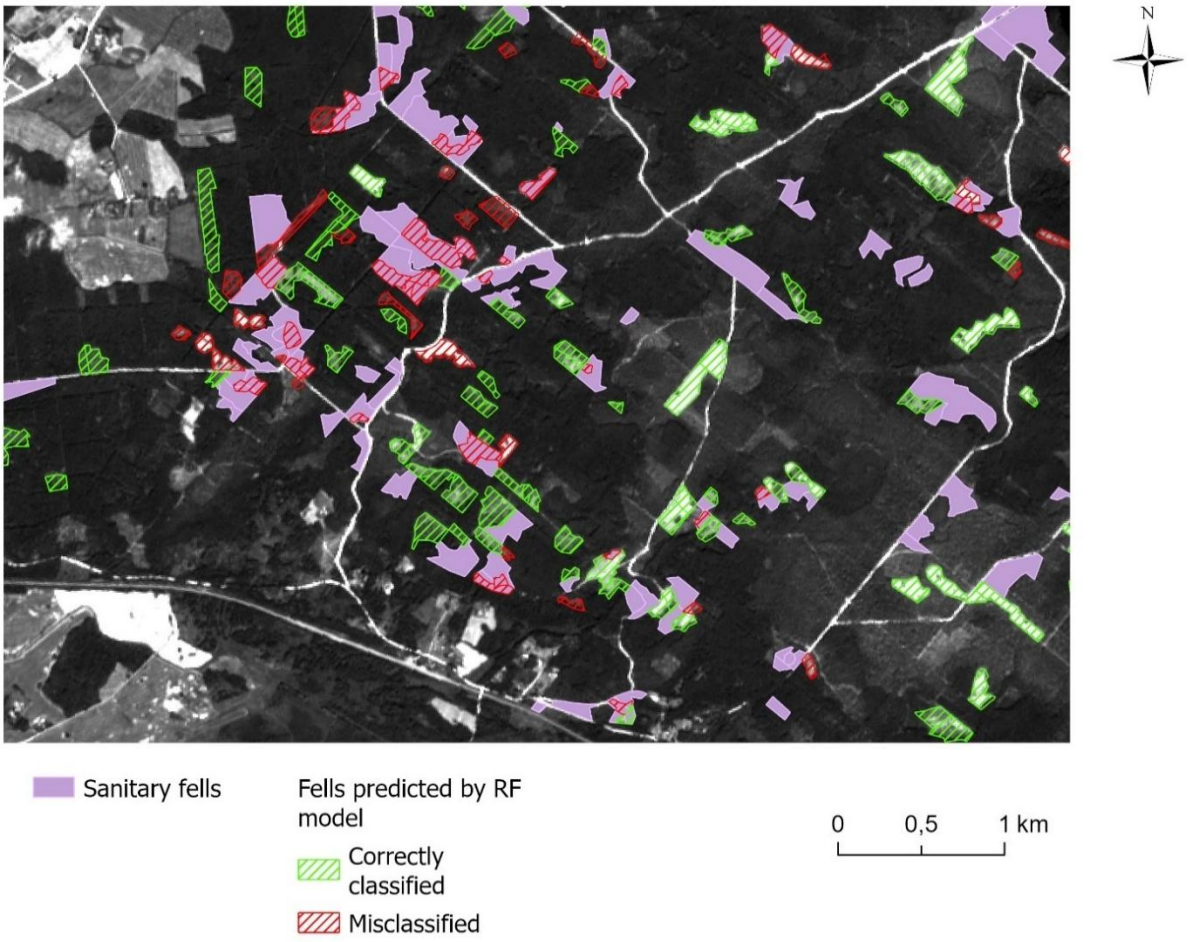

Figure 13. Misclassified clear-cut fells due to sanitary felling in Skaistkalne district.

As sanitary fells can have various felling degree and the model is tuned to detect the larger reflectance differences typical of clear-cut fells - some of the sanitary fells were identified as

clear-cut fells by the model. Attempts to include sanitary felling in the model training led to lower accuracy statistics. When the model was trained to detect fells in forest compartments using only clear-cuts, the classification performance was slightly better, with user accuracy of 0.74, producer accuracy of 0.73, and an F1 score of 0.73 (Table 8). However, when sanitary fells were added together with clear-cuts, the performance decreased, as indicated by lower user accuracy 0.72, producer accuracy 0.56 and F1 score 0.63 (Table 10). This suggests that the inclusion of sanitary fells increased classification confusion and indicates that the spectral signatures of sanitary fells differ from those of clear-cut felling.

Table 10. Random Forest model classification accuracy metrics when sanitary fells combined with clear-cuts.

	Results of model self-testing	Results of model unseen area testing
Overall accuracy	0.96	0.96
User's accuracy	0.80	0.72
Producer's accuracy	0.70	0.56
F1 score	0.75	0.63

4.4. Vegetation indices and their effectiveness in detecting clear-cut felling

When vegetation indices were added to the model, importance scores shows indices with moderately high importance scores (Figure 14). Among the indices, NDMI showed the highest importance score 0.393. Meanwhile, the importance of the visible bands 2 (blue) and 3 (green) have decreased when compared to results without indices (Figure 5).

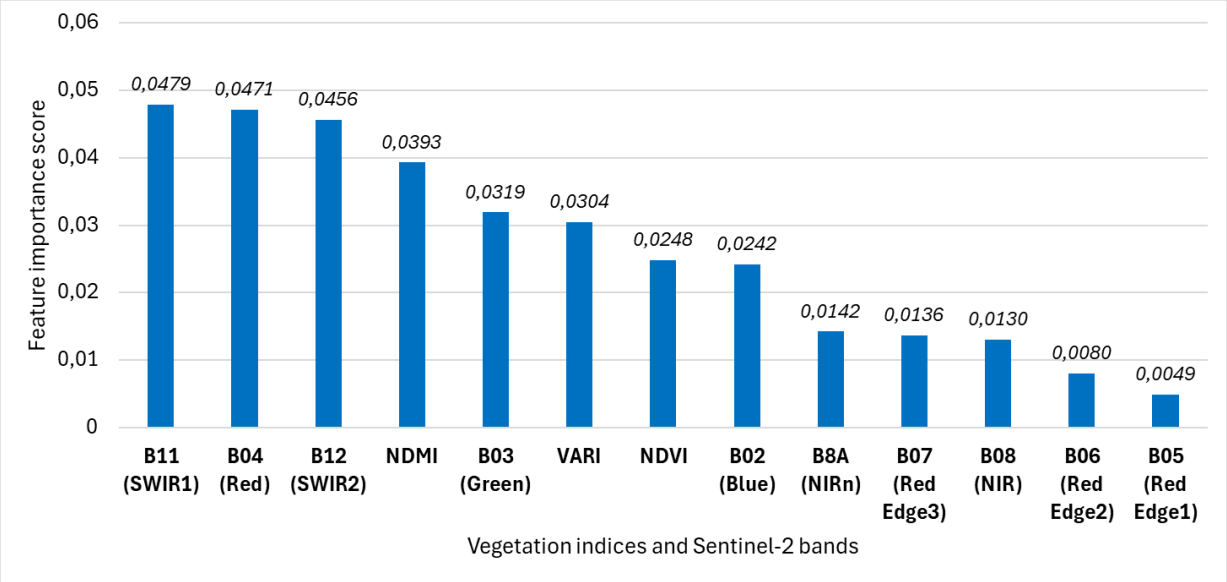

Figure 14. Importance scores of Sentinel-2 bands and vegetation indices for forest felling detection.

After adding indices data to the spectral band dataset, the RF model remained stable, showing similar results in self-testing with very small improvements in user accuracy (Figure 15).

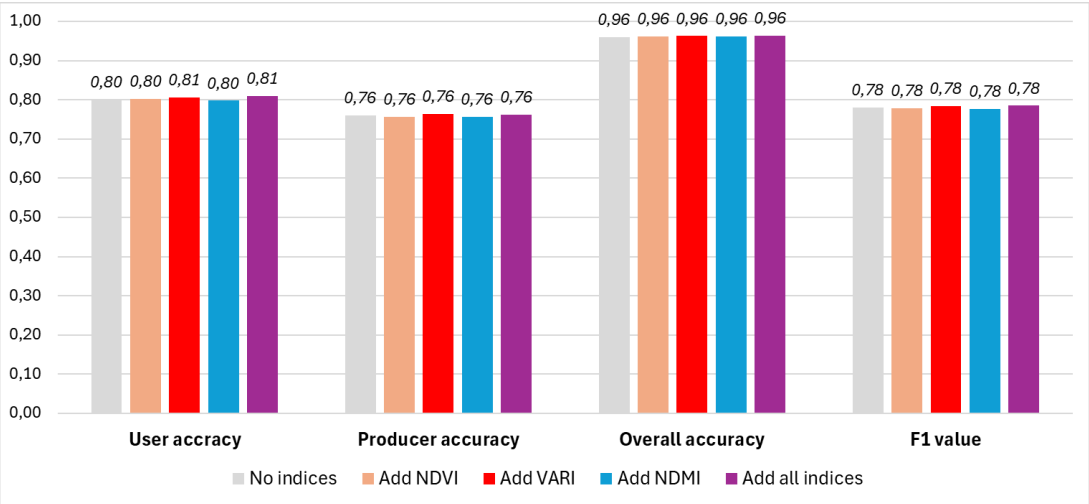

Figure 15. Random Forest model classification accuracy metrics with and without vegetation indices in model self-testing.

Tests on an unseen area show that the model is improved after adding vegetation indices (Figure 16). Among the individual indices, VARI showed highest improvement of all indices, increasing user accuracy by 3 %, producer accuracy by 4 %, overall accuracy by 1 % and F1 value by 4 %. Highest user accuracy was achieved when all indices were added, however highest producer accuracy 77 % was achieved when added VARI alone.

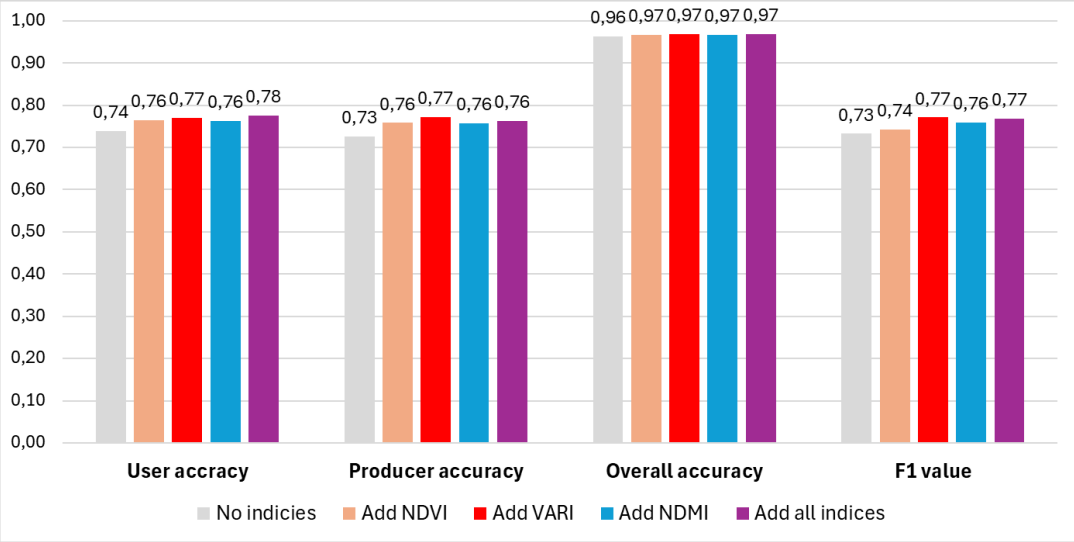

Figure 16. Random Forest model classification accuracy metrics with and without vegetation indices in unseen area testing.

5. Discussion

In this thesis, ML approach was performed to detect forest clear-cut fellings events from Sentinel-2 imagery. The methodology used in this study combined Sentinel-2 surface reflectance data with clear-cut historical felling events to generate training dataset for RF classification. The model performance was assessed using self-model testing and separate validation area unseen by model. The use of permutation-based feature importance by the RF provided insight of which spectral bands were most important to distinguish felled and non-felled compartments.

Calculation of median spectral difference on the forest compartment level instead of the pixel level has shown several advantages. It is less affected by noise in the data and studies have shown that it is more practical for operational use since forestry databases are based on compartments units (Molnár & Király, 2024). However, compartment-level mapping requires detailed and accurate forest compartment spatial data, which is feasible in Latvia, but may present challenges in other areas where data are missing.

Interpolation of Sentinel-2 data to a common resolution may have affected the results of study, because of spatial variability and altered edge responses. For compartment-level median aggregation, this influence is likely reduced, as it smooths individual extreme pixel values. Although, using nearest neighbor resampling instead of bilinear resampling could be possible option as it preserves the original reflectance values and maintains the discrete spatial structure of the satellite data (Fagundes et al., 2025). Another possible improvement could be applying undersampling to reduce the number of majority class (non-felled compartments) training samples and achieve a more balanced class distribution. However, according to (Douzas et al., 2019), undersampling may lead to loss of potentially useful information from the majority class and can increase model variance, which in some cases may also increase the risk of overfitting, particularly when the removed samples represent important spectral variability within the dominant class.

RF parameters, including class weighting and random state, were kept unchanged and were not extensively tuned in this study to ensure model reproducibility across different study areas and input feature combinations such as raw spectral bands and bands combined with vegetation indices. While additional hyperparameter optimization and class weighting experiments could potentially improve the detection of the minority class (fells) by enhancing recall and overall

F1 score, the objective of this study was to evaluate model stability rather than achieve maximum possible performance through parameter tuning.

Band importance results indicate that SWIR bands 11 and 12 are sensitive to forest felling, reflecting their responsiveness to changes in canopy moisture content and structural characteristics after harvesting. Red visible band shows second highest importance across spectral bands and it may be associated with reduced chlorophyll absorption following canopy removal (Hu et al., 2022). Although other study (Abdi, 2019) highlighted the high importance of NIR bands for detecting vegetation loss, particularly in boreal regions, the results of this study show that visible and SWIR bands exhibited stronger reflectance differences between felled and non-felled areas. The results suggest that, in the context of felling detection, spectral reflectance responses should not be interpreted as being driven by a single biophysical factor.

Band importance is influenced by multiple interacting environmental and structural conditions. Spectral responses may vary depending on tree species composition, branch, leaf structure and vegetation phenological stage (Genç & Altunel, 2025). Different species exhibit distinct canopy structures, pigment concentrations and moisture dynamics, which affects reflectance in visible, NIR and SWIR bands. Although images before and after felling were selected from the same season, they were acquired in different months across study areas, which may introduce phenological variability, as well as differences in sun position and atmospheric conditions, which can affect band reflectance (Schiller et al., 2024). Post-felling areas typically exhibit increased soil exposure and soil reflectance contributes to background spectral signals. The fells dataset covered a six-year period, meaning that some felling sites may contain older logging residues or regenerating young stands, whereas others represent more recent harvesting events with fresh cutting surfaces. These temporal and surface condition differences may further influence reflectance variability associated with felling detection.

When comparing band importance scores and spectral reflectance difference, bands with larger reflectance changes due to forest felling generally had higher importance scores in the RF model. Band 5 showed relatively high average reflectance difference due to felling, but it had the lowest band importance score. The reason for these results can be related to other bands competitiveness as there can be high correlation with other red edge bands (band 6 and 7). In addition, reflectance difference variance for band 5 across fells can affect the importance score as the RF favors features with stable class describing results (Belgiu & Drăguţ, 2016).

Achieving over 70% user and producer accuracy, F1 score in unseen-area testing, along with minimal differences compared to self-testing results, indicates that the model demonstrates stable performance under similar conditions. Similarity between user's and producer's accuracies indicates that model does not systematically under or overestimates fellings. Overall accuracy exceeded 95%, but this value should be interpreted cautiously as most of validated features were non-felled areas. In addition, generalizability assessment remains limited in this study. The district used in unseen area testing is located within Latvia and have same forest management practices, climatic conditions, temporal coverage and data source as the training areas. The results demonstrate spatial transferability within comparable ecological and forest management areas. However, additional validation across more heterogeneous regions and varying environmental conditions is necessary to confirm the robustness and broader applicability of the model beyond Latvia.

The results showed that the majority of RF model overclassifications are associated with sanitary felling, which accounts for approximately 79 % of all overestimated felling detections. Classification patterns showed strong changes in visible and SWIR bands for overestimated fellings, which are linked to sanitary, reconstructive and thinning fellings, where partial canopy removal triggers clear-cut signatures. These patterns also align with classification results analyzed by dominant forest compartment species – spruce dominated compartments accounts for the highest overestimation of fellings, and sanitary fellings are most frequent in these compartments due to spruce bark beetle damages. Classification performed well in pine, birch and aspen dominated compartments, but the lowest performance were in gray alder compartments, which is related to the small number of compartments where it is dominant species. Results showed that the reflectance difference after a clear-cut event can range from 30 to 100 spectral units in the red band, which is a relatively large variation that can sometimes make it more difficult for the model to accurately classify changes. On the other hand, missed fellings (FN) showed lower reflectance differences than actual fells (TP), causing model to misclassify these forest compartments as fells. Results showed better classification statistics for larger compartments as greater area produces more stable and reliable spectral data for classification algorithms.

Some of the misclassified compartments were affected by clouds in Sentinel-2 images. Although SCL layer was used to cover cloudy areas, some of the nearest pixels still were affected by clouds and had extreme reflectance values due to basic SCL-based cloud masking approach. Possible improvements could be masking pixels around SCL layer and masking

edges of forest compartments to reduce mixed pixels near boundaries. Another solution could be screening these extreme values before median calculation.

Addition of vegetation indices data to the RF model provided meaningful insights. The model self-testing results were almost the same as those obtained without vegetation indices, which may be explained by the limited testing data and the fact that the indices were derived from the same underlying Sentinel-2 spectral bands. These factors reduce the sensitivity of the model to small changes from additional indices. Moreover, training and test samples originated from the same forest areas, limiting variability.

In the band importance analysis, the indices ranked in the middle of ranking, because the strongest spectral bands already provided most of the discriminative power. Furthermore, since the indices are computed from these same bands, the model tends to rely on the indices, which can reduce the importance of the original bands.

However, testing on an unseen area showed that indices improved model performance. Each index contributed 1-4 % improvements on all accuracy metrics – largest differences identified in user accuracy (74 % without indices and 78 % with all indices together) and producer accuracy (73 % without indices and 77 % with VARI). Among the three indices, VARI provided slightly better improvements, likely due its band formula – it uses only visible bands 2 (blue), 3 (green), 4 (red), which were already among the most important bands before indices were added. Although another study (Nugraha et al., 2024) reports NDVI as more accurate and sensitive index in vegetation monitoring compared to VARI, lower results of NDVI can be described with overclassifications – it is more sensitive to vegetation changes and it can more often overclassify sanitary fells as clear-cuts. NDMI also performed well, reflecting moisture loss after forest felling and the importance of band 11 (SWIR1) in such clear-cut identification.

Since the vegetation indices used in this study are mathematical transformations of the original spectral bands, they introduce additional correlated predictors rather than entirely new independent information. When indices were included in the model, the importance of some original bands, such as the green and blue visible bands, decreased, while others remained relatively stable. This pattern can be explained by multicollinearity effect in RF model. When multiple predictors encode similar information, there can be correlation between features that creates noises in datasets, affecting prediction accuracy (Dobrinic et al., 2022). Importantly, such correlation does not necessarily reduce predictive performance, as RF can successfully handle high data multicollinearity (Belgiu & Drăguţ, 2016). Findings show that correlation do

not reduced predictive accuracy strongly, but effected band variable importance interpretation. Although vegetation indices do not provide additional raw spectral data, their normalized transformation structure helps mitigate variability associated with environmental factors such as seasonal phenological changes and atmospheric scattering effect limitations, for example, VARI index design to minimize atmospheric effects (Gitelson et al., 2002). The improvements of accuracies in spatially independent validation suggest that vegetation indices contribute to improved model robustness and generalization rather than substantially increasing separability within the training data.

Findings from this study demonstrate that Sentinel-2 based clear-cut detection using the RF method can be successfully used to monitor harvesting activities. It can be used to validate logging areas remotely or to identify unmapped clear-cuts from historical Sentinel-2 data. Additional potential applications include military intelligence, where such methods could help identify early signs of military installations.

6. Conclusions

This study showed that the integration of Sentinel-2 imagery and machine learning (ML) algorithm like Random Forest (RF) offers a reliable method for detecting forest clear-cut felling events in Latvia. By analyzing Sentinel-2 imagery spectral data before and after historical felling events, the model demonstrated capabilities of distinguishing felled and non-felled forest compartments. Testing on an independent forest district achieved an overall accuracy exceeding 95%, with producer and user accuracies of 73% and 74%, respectively.

Evaluation of Sentinel-2 spectral band importance indicates that red (band 4) and short-wave infrared (bands 11, 12) were most effective for identifying forest felling. In contrast, red-edge (bands 5, 6, 7) and near-infrared (NIR) (bands 8, 8A) contributed less to classification, while other visible bands like blue (band 2) and green (band 3) showed stable and moderate performance.

The analysis of the model performance by forest compartment size and dominant tree species highlighted larger compartments as more stable and accurate to classification, while smaller compartments and spruce dominated stands were more prone to classification errors. Cloud-affected pixels and partial canopy removal fell types, especially, sanitary fells, were identified as key sources of misclassification.

Integrating vegetation indices into the RF model resulted in slight, but meaningful improvements in accuracies. Visible Atmospherically Resistant Index (VARI) provided the greatest improvements when compared to Normalized Difference Vegetation Index (NDVI) and Normalized Difference Moisture Index (NDMI) with user and producer accuracies achieving 77 %, which is 3-4 % improvements when compared to results without any indices data. Similar results achieved when adding all 3 indices together with raw band data.

Overall, this research highlights the practical usefulness of Sentinel-2 satellite data and the RF classification method for monitoring forest felling in Latvia. However, further validation in more diverse ecological and management conditions is required to confirm the robustness and broader applicability of the method beyond the study region. The results may have been influenced by preprocessing procedures, including interpolation of Sentinel-2 imagery to a common spatial resolution, which may introduce smoothing effects and alter edge responses. Spectral variability may also be affected by temporal differences between image acquisitions, species composition differences in Latvia, and the extended study period, during which logging

residues, regeneration processes, and phenological changes could influence reflectance signals. These factors should be considered when interpreting the reported classification performance.

References

Abdi, A., M. (2019). Land cover and land use classification performance of machine learning algorithms in a boreal landscape using Sentinel-2 data. *GIScience & Remote Sensing*. 57(1), 1-20. https://doi.org/10.1080/15481603.2019.1650447

Belgiu, M. & Drăguţ, L. (2016). Random forest in remote sensing: A review of applications and future directions. *Journal of Photogrammetry and Remote Sensing*. 114. 24-31. https://doi.org/10.1016/j.isprsjprs.2016.01.011

Calders, K., Jonckheere, I., Nightingale, J., Vastaranta, M. (2020). Remote Sensing Technology Applications in Forestry and REDD+. *Forests*. 11(2). 188. https://doi.org/10.3390/f11020188

Central Statistical Bureau of Latvia. (2024). *Planned felling volume indicated in tree felling licence by type of felling.* https://stat.gov.lv/en/statistics-themes/business-sectors/forestry/tables/mez020c-planned-felling-volume-indicated-tree

Cimdiņš, R. (2018). *Sentinel-1 izmantošanas iespējas mežsaimnieciskās darbības kontrolē.* https://dspace.lu.lv/items/c0ed2632-4ccf-410a-b1d9-ca90f197a6d0

Clevers, J., Gitelson, A. (2013). Remote estimation of crop and grass chlorophyll and nitrogen content using red-edge bands on Sentinel-2 and -3. *International Journal of Applied Earth Observation and Geoinformation.* 23. 344-351. https://doi.org/10.1016/j.jag.2012.10.008

Dobrinic, D., Gasparovic, M., Damir, M. (2022). Evaluation of feature selection methods for vegetation mapping using multitemporal Sentinel imagery. *The International Archives of the Photogrammetry, Remote Sensing and Spatial Information Sciences.* 485-491. https://doi.org/10.5194/isprs-archives-XLIII-B3-2022-485-2022

Douzas, G., Bacao, F., Fonseca, J., Khudinyan, M. (2019). Imbalanced Learning in Land Cover Classification: Improving Minority Classes Prediction Accuracy Using the Geometric SMOTE Algorithm. *Remote Sensing*. 11(24), 3040. https://doi.org/10.3390/rs11243040

Envirotech. (2021). *GIS Latvija 10.2.* https://www.gisbaltic.eu/content/dam/distributor-restricted/gisbaltic-eu/esri-lv/apmacibas/gislatvija10.2.zip

ESRI. (2025). *Accuracy assessment*. https://pro.arcgis.com/en/pro-app/latest/help/analysis/image-analyst/accuracy-assessment.htm

Fagundes, R., Kayser, L. P., de Paula Amaral, L., Benedetti, A. C., Bolfe, É. L., Parreiras, T. C., Ramos-Ospina, M., Marulanda-Tobón, A. (2025). Analysis of Resampling Methods for the Red Edge Band of MSI/Sentinel-2A for Coffee Cultivation Monitoring. *Geomatics*, 5(2), 19. https://doi.org/10.3390/geomatics5020019

Fassnacht, F. E., White, J. C., Wulder, M. A., Naesset, E. (2024). Remote sensing in forestry: current challenges, considerations and directions. *Forestry: An International Journal of Forest Research*. 97. 11-37. https://doi.org/10.1093/forestry/cpad024

Francini, S., Schelhaas, M., J., Vangi, E., Lerink, B., Nabuurs, G., J., McRoberts, R., E., Chirici, G. (2024). Forest species mapping and area proportion estimation combining Sentinel-2 harmonic predictors and national forest inventory data. *International Journal of Applied Earth Observation and Geoinformation*. 131. 103935. https://doi.org/10.1016/j.jag.2024.103935

Gao, B., C. (1996). NDWI—A normalized difference water index for remote sensing of vegetation liquid water from space. *Remote Sensing of Environment*. 58(3). 257-266. https://doi.org/10.1016/S0034-4257(96)00067-3

Genç, Ç., Ö., Altunel, A., O. (2025). Monitoring the operational changes in surface reflectances after logging, based on popular indices over Sentinel-2, Landsat-8, and ASTER imageries. E*nvironmental Monitoring and Assessment.* 197(120). 1-17. https://doi.org/10.1007/s10661-024-13526-w

Gitelson, A., Stark, R., Grits, U., Rundquist, D., Kaufman, Y., Derry, D. (2002). Vegetation and soil lines in visible spectral space: A concept and technique for remote estimation of vegetation fraction. *International Journal for Remote Sensing.* 23(13). 2537-2562. https://doi.org/10.1080/01431160110107806

Hu, Y., Wang, Z., Zhang, Y., Dian, Y. (2022). Logging Pattern Detection by Multispectral Remote Sensing Imagery in North Subtropical Plantation Forests. *Remote Sensing*. 14 (19). 4987. https://doi.org/10.3390/rs14194987

Huete, A., R. (1988). A soil-adjusted vegetation index (SAVI). *Remote Sensing of Environment* 25 (3), 295-309. https://doi.org/10.1016/0034-4257(88)90106-X

Hunt, E., R., Rock, B., N. (1989). Detection of changes in leaf water content using Near and Middle-Infrared reflectance. *Remote Sensing of Environment*. 30(1). 43-54. https://doi.org/10.1016/0034-4257(89)90046-1

Immitzer, M., Vuolo, F., Atzberger, C. (2016). First Experience with Sentinel-2 Data for Crop and Tree Species Classifications in Central Europe. *Remote Sensing.* 8. 166. http://dx.doi.org/10.3390/rs8030166

Laiviņš, O. (2018). Latvijas ainavzemes un ainavapvidi. Nikodemus, O., Kļaviņš, M., Krišjāne, Z., Zelčs, V. LATVIJA. ZEME, DABA, TAUTA, VALSTS. Rīga, Latvijas Universitātes Akadēmiskais apgāds, 424-428.

Latvian State Forests. (2024). *Forest Management Plan public share.* https://www.lvm.lv/images/lvm/sabiedribai/meza-apsaimniekosanas-plani/meza-apsaimniekosanas-plana-publiska-dala.pdf

Latvian State Forests. (2025). *Latvia's State Forests Develops an Algorithm for Damage Detection in Spruce Stands.* https://www.researchlatvia.gov.lv/en/latvias-state-forests-develops-algorithm-damage-detection-spruce-stands

Latvian Forest Development Fund. (2025). *Latvian forest sector in facts & figures*. https://mezaskaitli.lv/en

Lechner, A. M., Foody, G. M., Boyd, D., S. (2020). Applications in Remote Sensing to Forest Ecology and Management. *One Earth*. 2. 405-412. https://doi.org/10.1016/j.oneear.2020.05.001

Lewińska, K., E., Ernst, S., Frantz, D., Leser, U., Hostert, P. (2024). Global overview of usable Landsat and Sentinel-2 data for 1982–2023. *Data in Brief*. 57. 111054. https://doi.org/10.1016/j.dib.2024.111054

LVM GEO. (2025). *Open spatial data*. https://www.lvmgeo.lv/en/data

Manjunath, K., R., Kumar, A., Meenakshi, M., Renu, R., Uniyal. S., K., Singh, R., D., Ahuja, P.,S., Ray, S., S., Panigrahy, S. (2014). Developing Spectral Library of Major Plant Species of Western Himalayas Using Ground Observations. *Journal of the Indian Society of Remote Sensing*. 42. 205. http://dx.doi.org/10.1007/s12524-013-0305-0

Massey, R., Berner, L.T., Foster, A.C., Goetz, S.J., Vepakomma, U. (2023). Remote Sensing Tools for Monitoring Forests and Tracking Their Dynamics. In: Girona, M. M., Morin, H., Gauthier, S., Bergeron, Y. (eds) *Boreal Forests in the Face of Climate Change. Advances in Global Change Research*. 74. 637-643. Springer. https://link.springer.com/chapter/10.1007/978-3-031-15988-6_26

Mikeladze, G., Gavashelishvili, A., Akobia, I., Metreveli, V. (2020). Estimation of forest cover change using Sentinel-2 multi-spectral imagery in Georgia (the Caucasus). *iForest - Biogeosciences and Forestry*. 13. 329-335. https://iforest.sisef.org/abstract/?id=ifor3386-013

Minunno, F., Miettinen, J., Tian, X., Häme, T., Holder, J., Koivu, K., Mäkelä, A. (2025). Data assimilation of forest status using Sentinel-2 data and a process-based model. *Agricultural and Forest Meteorology*. 363. 110436. https://linkinghub.elsevier.com/retrieve/pii/S0168192325000565

Mohammadpour, P., Viegas, D., X., Viegas, C. (2022). Vegetation Mapping with Random Forest Using Sentinel 2 and GLCM Texture Feature – A Case Study for Lousã Region, Portugal. *Remote Sensing*. 14. 4585. https://www.mdpi.com/2072-4292/14/18/4585

Molnár, T., & Király, G. (2024). Forest Disturbance Monitoring Using Cloud-Based Sentinel-2 Satellite Imagery and Machine Learning. *Journal of Imaging*. 10, 14. https://www.mdpi.com/2313-433X/10/1/14

Nelson, M., D., McRoberts, R., E., Holden, G., R., Bauer, M., E. 2009. Effects of satellite image spatial aggregation and resolution on estimates of forest land area. *International Journal of Remote Sensing*. 30(8). 1913-1940. https://doi.org/10.1080/01431160802545631

Noi, P. T., Kappas, M. (2017). Comparison of Random Forest, k-Nearest Neighbor, and Support Vector Machine Classifiers for Land Cover Classification Using Sentinel-2 Imagery. *Sensors*. 18, 18. https://doi.org/10.3390/s18010018

Nugraha, M. G., Widyawati, L. M. S., Maulana, A., Yulianto, K. R. (2024). Application of NDVI and VARI in Vegetation Monitoring Using GIS and Remote Sensing on Patuha Geothermal Area. In *PROCEEDINGS, The 10th Indonesia International Geothermal Convention & Exhibition (IIGCE) 2024.* https://www.researchgate.net/publication/384269036_Application_of_NDVI_and_VARI_in_Vegetation_Monitoring_Using_GIS_and_Remote_Sensing_on_Patuha_Geothermal_Area

Pandey, P. & Arellano, P. (2022). *Advances in Remote Sensing for Forest Monitoring*. 5. John Wiley & Sons Ltd. 5.

Pelc-Mieczkowska, R. (2021). The Application of Sentinel-2 Data for Automatic Forest Cover Changes Assessment – Białowieża Primeval Forest Case Study. *Civil and Environmental Engineering Reports*. 31. 148-166. http://dx.doi.org/10.2478/ceer-2021-0054

Pelletier, C., Valero, S., Inglada, J., Champion, N., Marais Sicre, C., & Dedieu, G. (2017). Effect of Training Class Label Noise on Classification Performances for Land Cover Mapping with Satellite Image Time Series. *Remote Sensing*. 9(2). 173. https://doi.org/10.3390/rs9020173

Penuelas, J., Baret, F., Filella, I. (1995). Semi-Empirical Indices to Assess Carotenoids/Chlorophyll-a Ratio from Leaf Spectral Reflectance. *Photosynthetica*. 31. 221-230. https://www.researchgate.net/publication/229084513

Pour, A., B., Ranjbar, H., Sekandari, M., El-Wahed, M., A., Hossain, M., S., Hashim, M., Yousefi, M., Zoheir, B., Wambo, J., D., T., Muslim, A., M. (2023). Remote sensing for mineral exploration. *Geospatial Analysis Applied to Mineral Exploration*. 33. https://doi.org/10.1016/B978-0-323-95608-6.00002-0

Rozentāls, G., Daugaviete, M., Lazdāns, V., Liepiņš, K., Šmits, A., Zaļuma, A., Zariņa, I. (2017). *Kas jāzina meža īpašniekam*. Edited by I. Konstantinova. Latvijas Valsts mežzinātnes institūts Silava. Biedrība Meža īpašnieku kooperācijas atbalsta centrs.

SAS. (2025). *A guide to the types of machine learning algorithms and their applications*. https://www.sas.com/en_gb/insights/articles/analytics/machine-learning-algorithms.html

Schiller, C., Költzow, J., Schwarz, S., Schiefer, F., Fassnacht, F., E. (2024). Forest disturbance detection in Central Europe using transformers and Sentinel-2 time series. *Remote Sensing of Environment.* 315. 114475. https://doi.org/10.1016/j.rse.2024.114475

Scikit-learn developers. (2025). *User guide*. https://scikit-learn.org/stable/user_guide.html

Silava. (2025). *Latvijas zemes izmantošanas, zemes izmantošanas maiņas un mežsaimniecības (ZIZIMM) sektora klimata pārmaiņu mazināšanas mērķu sasniegšanai īstenojamo darbību siltumnīcefekta gāzu (SEG) emisiju mazināšanai un oglekļa dioksīda (CO_2) piesaistes veicināšanai meža apsaimniekošanā: sociāli ekonomiskais vērtējums.* https://www.silava.lv/images/Petijumi/2025-ZM-25-00-S0INZ03-00027-ZIZIMM/2025-ZM-LAD-25-00-S0INZ03-000027-ZIZIMM-Parskats.pdf

Slagter, B., Reiche, J., Marcos, D., Mullissa, A. (2023). Monitoring direct drives of small-scale tropical forest disturbance in near real-time with Sentinel-1 and -2 data. *Remote sensing of Environment.* 1-17. 295. https://doi.org/10.1016/j.rse.2023.113655

Sobrino, J., A., Llorens, R., Fernandez, C., Fernandez-Alonso, J., Vega, J., A. (2024). Methodology for burned areas delimitation and fire severity assessment using Sentinel-2 data. A case study of forest fires occurred in Spain between 2018 and 2023. *Recent advances in Remote Sensing.* 1-13. http://dx.doi.org/10.62880/rars240002

SOCR. (2025). *Data Science and Predictive Analytics. Evaluating model performance.* https://www.socr.umich.edu/people/dinov/2017/Spring/DSPA_HS650/notes/13_ModelEvaluation.html

Spadoni, G., L., Cavalli, A., Congedo, L., Munafò, M. (2020). Analysis of Normalized Difference Vegetation Index (NDVI) multi-temporal series for the production of forest cartography. *Remote Sensing Applications: Society and Environment.* 20. 1-12. https://doi.org/10.1016/j.rsase.2020.100419

Upreti, A. (2022). Machine Learning Application in GIS and Remote Sensing: An overview. *Preprints.* http://dx.doi.org/10.20944/preprints202207.0302.v1

Yang, L., Haokui, Z., Xizhe, X., Yenan, J., Qiang, S. (2018). Deep learning for remote sensing image classification: A survey. *Wiley Interdisciplinary Reviews: Data Mining and Knowledge Discovery.* 8(12). 1-17. https://doi.org/10.1002/widm.1264

Zhang, X., Shen, H., Huang, T., Wu, Y., Guo, B., Liu, Z., Luo, H., Tang, J., Zhou, H., Wang, L., Xu, W., Ou, G. (2024). Improved random forest algorithms for increasing the accuracy of forest aboveground biomass estimation using Sentinel-2 imagery. *Ecological Indicators*. 159. 111752. https://doi.org/10.1016/j.ecolind.2024.111752

Zhangyan, J., Huete, A., R., Didan, K., Tomoaki, M. (2008). Development of a two-band enhanced vegetation index without a blue band. *Remote Sensing of Environment*. 112 (10). 3833-3845. https://doi.org/10.1016/j.rse.2008.06.006

Appendices

Python script for mapping fells from Sentinel-2 data

https://gitlab.com/gk4382352/python/-/blob/main/Sentinel2FellMapper.py

Series from Lund University

Department of Physical Geography and Ecosystem Science

Master Thesis in Geographical Information Science

1. *Anthony Lawther:* The application of GIS-based binary logistic regression for slope failure susceptibility mapping in the Western Grampian Mountains, Scotland (2008).
2. *Rickard Hansen:* Daily mobility in Grenoble Metropolitan Region, France. Applied GIS methods in time geographical research (2008).
3. *Emil Bayramov:* Environmental monitoring of bio-restoration activities using GIS and Remote Sensing (2009).
4. *Rafael Villarreal Pacheco:* Applications of Geographic Information Systems as an analytical and visualization tool for mass real estate valuation: a case study of Fontibon District, Bogota, Columbia (2009).
5. *Siri Oestreich Waage:* a case study of route solving for oversized transport: The use of GIS functionalities in transport of transformers, as part of maintaining a reliable power infrastructure (2010).
6. *Edgar Pimiento:* Shallow landslide susceptibility – Modelling and validation (2010).
7. *Martina Schäfer:* Near real-time mapping of floodwater mosquito breeding sites using aerial photographs (2010).
8. *August Pieter van Waarden-Nagel:* Land use evaluation to assess the outcome of the programme of rehabilitation measures for the river Rhine in the Netherlands (2010).
9. *Samira Muhammad:* Development and implementation of air quality data mart for Ontario, Canada: A case study of air quality in Ontario using OLAP tool. (2010).
10. *Fredros Oketch Okumu*: Using remotely sensed data to explore spatial and temporal relationships between photosynthetic productivity of vegetation and malaria transmission intensities in selected parts of Africa (2011).
11. *Svajunas Plunge:* Advanced decision support methods for solving diffuse water pollution problems (2011).
12. *Jonathan Higgins:* Monitoring urban growth in greater Lagos: A case study using GIS to monitor the urban growth of Lagos 1990 - 2008 and produce future growth prospects for the city (2011).
13. *Mårten Karlberg:* Mobile Map Client API: Design and Implementation for Android (2011).

14. *Jeanette McBride:* Mapping Chicago area urban tree canopy using color infrared imagery (2011).

15. *Andrew Farina:* Exploring the relationship between land surface temperature and vegetation abundance for urban heat island mitigation in Seville, Spain (2011).

16. *David Kanyari*: Nairobi City Journey Planner: An online and a Mobile Application (2011).

17. *Laura V. Drews:* Multi-criteria GIS analysis for siting of small wind power plants - A case study from Berlin (2012).

18. *Qaisar Nadeem:* Best living neighborhood in the city - A GIS based multi criteria evaluation of ArRiyadh City (2012).

19. *Ahmed Mohamed El Saeid Mustafa:* Development of a photo voltaic building rooftop integration analysis tool for GIS for Dokki District, Cairo, Egypt (2012).

20. *Daniel Patrick Taylor*: Eastern Oyster Aquaculture: Estuarine Remediation via Site Suitability and Spatially Explicit Carrying Capacity Modeling in Virginia's Chesapeake Bay (2013).

21. *Angeleta Oveta Wilson:* A Participatory GIS approach to *unearthing* Manchester's Cultural Heritage '*gold mine'* (2013).

22. *Ola Svensson:* Visibility and Tholos Tombs in the Messenian Landscape: A Comparative Case Study of the Pylian Hinterlands and the Soulima Valley (2013).

23. *Monika Ogden:* Land use impact on water quality in two river systems in South Africa (2013).

24. *Stefan Rova:* A GIS based approach assessing phosphorus load impact on Lake Flaten in Salem, Sweden (2013).

25. *Yann Buhot:* Analysis of the history of landscape changes over a period of 200 years. How can we predict past landscape pattern scenario and the impact on habitat diversity? (2013).

26. *Christina Fotiou:* Evaluating habitat suitability and spectral heterogeneity models to predict weed species presence (2014).

27. *Inese Linuza:* Accuracy Assessment in Glacier Change Analysis (2014).

28. *Agnieszka Griffin:* Domestic energy consumption and social living standards: a GIS analysis within the Greater London Authority area (2014).

29. *Brynja Guðmundsdóttir:* Detection of potential arable land with remote sensing and GIS - A Case Study for Kjósarhreppur (2014).

30. *Oleksandr Nekrasov:* Processing of MODIS Vegetation Indices for analysis of agricultural droughts in the southern Ukraine between the years 2000-2012 (2014).

31. *Sarah Tressel:* Recommendations for a polar Earth science portal in the context of Arctic Spatial Data Infrastructure (2014).

32. *Caroline Gevaert:* Combining Hyperspectral UAV and Multispectral Formosat-2 Imagery for Precision Agriculture Applications (2014).

33. *Salem Jamal-Uddeen:* Using GeoTools to implement the multi-criteria evaluation analysis - weighted linear combination model (2014).

34. *Samanah Seyedi-Shandiz:* Schematic representation of geographical railway network at the Swedish Transport Administration (2014).

35. *Kazi Masel Ullah:* Urban Land-use planning using Geographical Information System and analytical hierarchy process: case study Dhaka City (2014).

36. *Alexia Chang-Wailing Spitteler:* Development of a web application based on MCDA and GIS for the decision support of river and floodplain rehabilitation projects (2014).

37. *Alessandro De Martino:* Geographic accessibility analysis and evaluation of potential changes to the public transportation system in the City of Milan (2014).

38. *Alireza Mollasalehi:* GIS Based Modelling for Fuel Reduction Using Controlled Burn in Australia. Case Study: Logan City, QLD (2015).

39. *Negin A. Sanati:* Chronic Kidney Disease Mortality in Costa Rica; Geographical Distribution, Spatial Analysis and Non-traditional Risk Factors (2015).

40. *Karen McIntyre:* Benthic mapping of the Bluefields Bay fish sanctuary, Jamaica (2015).

41. *Kees van Duijvendijk:* Feasibility of a low-cost weather sensor network for agricultural purposes: A preliminary assessment (2015).

42. *Sebastian Andersson Hylander:* Evaluation of cultural ecosystem services using GIS (2015).

43. *Deborah Bowyer:* Measuring Urban Growth, Urban Form and Accessibility as Indicators of Urban Sprawl in Hamilton, New Zealand (2015).

44. *Stefan Arvidsson:* Relationship between tree species composition and phenology extracted from satellite data in Swedish forests (2015).

45. *Damián Giménez Cruz*: GIS-based optimal localisation of beekeeping in rural Kenya (2016).

46. *Alejandra Narváez Vallejo:* Can the introduction of the topographic indices in LPJ-GUESS improve the spatial representation of environmental variables? (2016).

47. *Anna Lundgren:* Development of a method for mapping the highest coastline in Sweden using breaklines extracted from high resolution digital elevation models (2016).

48. *Oluwatomi Esther Adejoro:* Does location also matter? A spatial analysis of social achievements of young South Australians (2016).

49. *Hristo Dobrev Tomov:* Automated temporal NDVI analysis over the Middle East for the period 1982 - 2010 (2016).

50. *Vincent Muller:* Impact of Security Context on Mobile Clinic Activities A GIS Multi Criteria Evaluation based on an MSF Humanitarian Mission in Cameroon (2016).

51. *Gezahagn Negash Seboka:* Spatial Assessment of NDVI as an Indicator of Desertification in Ethiopia using Remote Sensing and GIS (2016).

52. *Holly Buhler:* Evaluation of Interfacility Medical Transport Journey Times in Southeastern British Columbia. (2016).

53. *Lars Ole Grottenberg*: Assessing the ability to share spatial data between emergency management organisations in the High North (2016).

54. *Sean Grant:* The Right Tree in the Right Place: Using GIS to Maximize the Net Benefits from Urban Forests (2016).

55. *Irshad Jamal:* Multi-Criteria GIS Analysis for School Site Selection in Gorno-Badakhshan Autonomous Oblast, Tajikistan (2016).

56. *Fulgencio Sanmartín:* Wisdom-volkano: A novel tool based on open GIS and time-series visualization to analyse and share volcanic data (2016).

57. *Nezha Acil:* Remote sensing-based monitoring of snow cover dynamics and its influence on vegetation growth in the Middle Atlas Mountains (2016).

58. *Julia Hjalmarsson:* A Weighty Issue: Estimation of Fire Size with Geographically Weighted Logistic Regression (2016).

59. *Mathewos Tamiru Amato:* Using multi-criteria evaluation and GIS for chronic food and nutrition insecurity indicators analysis in Ethiopia (2016).

60. *Karim Alaa El Din Mohamed Soliman El Attar:* Bicycling Suitability in Downtown, Cairo, Egypt (2016).

61. *Gilbert Akol Echelai:* Asset Management: Integrating GIS as a Decision Support Tool in Meter Management in National Water and Sewerage Corporation (2016).

62. *Terje Slinning:* Analytic comparison of multibeam echo soundings (2016).

63. *Gréta Hlín Sveinsdóttir:* GIS-based MCDA for decision support: A framework for wind farm siting in Iceland (2017).

64. *Jonas Sjögren:* Consequences of a flood in Kristianstad, Sweden: A GIS-based analysis of impacts on important societal functions (2017).

65. *Nadine Raska:* 3D geologic subsurface modelling within the Mackenzie Plain, Northwest Territories, Canada (2017).

66. *Panagiotis Symeonidis*: Study of spatial and temporal variation of atmospheric optical parameters and their relation with PM 2.5 concentration over Europe using GIS technologies (2017).

67. *Michaela Bobeck:* A GIS-based Multi-Criteria Decision Analysis of Wind Farm Site Suitability in New South Wales, Australia, from a Sustainable Development Perspective (2017).

68. *Raghdaa Eissa*: Developing a GIS Model for the Assessment of Outdoor Recreational Facilities in New Cities Case Study: Tenth of Ramadan City, Egypt (2017).

69. *Zahra Khais Shahid*: Biofuel plantations and isoprene emissions in Svea and Götaland (2017).

70. *Mirza Amir Liaquat Baig*: Using geographical information systems in epidemiology: Mapping and analyzing occurrence of diarrhea in urban - residential area of Islamabad, Pakistan (2017).

71. *Joakim Jörwall*: Quantitative model of Present and Future well-being in the EU-28: A spatial Multi-Criteria Evaluation of socioeconomic and climatic comfort factors (2017).

72. *Elin Haettner*: Energy Poverty in the Dublin Region: Modelling Geographies of Risk (2017).

73. *Harry Eriksson*: Geochemistry of stream plants and its statistical relations to soil- and bedrock geology, slope directions and till geochemistry. A GIS-analysis of small catchments in northern Sweden (2017).

74. *Daniel Gardevärn:* PPGIS and Public meetings – An evaluation of public participation methods for urban planning (2017).

75. *Kim Friberg:* Sensitivity Analysis and Calibration of Multi Energy Balance Land Surface Model Parameters (2017).

76. *Viktor Svanerud:* Taking the bus to the park? A study of accessibility to green areas in Gothenburg through different modes of transport (2017).

77. *Lisa-Gaye Greene*: Deadly Designs: The Impact of Road Design on Road Crash Patterns along Jamaica's North Coast Highway (2017).

78. *Katarina Jemec Parker*: Spatial and temporal analysis of fecal indicator bacteria concentrations in beach water in San Diego, California (2017).

79. *Angela Kabiru*: An Exploratory Study of Middle Stone Age and Later Stone Age Site Locations in Kenya's Central Rift Valley Using Landscape Analysis: A GIS Approach (2017).

80. *Kristean Björkmann*: Subjective Well-Being and Environment: A GIS-Based Analysis (2018).

81. *Williams Erhunmonmen Ojo*: Measuring spatial accessibility to healthcare for people living with HIV-AIDS in southern Nigeria (2018).

82. *Daniel Assefa*: Developing Data Extraction and Dynamic Data Visualization (Styling) Modules for Web GIS Risk Assessment System (WGRAS). (2018).

83. *Adela Nistora*: Inundation scenarios in a changing climate: assessing potential impacts of sea-level rise on the coast of South-East England (2018).

84. *Marc Seliger*: Thirsty landscapes - Investigating growing irrigation water consumption and potential conservation measures within Utah's largest master-planned community: Daybreak (2018).

85. *Luka Jovičić*: Spatial Data Harmonisation in Regional Context in Accordance with INSPIRE Implementing Rules (2018).

86. *Christina Kourdounouli*: Analysis of Urban Ecosystem Condition Indicators for the Large Urban Zones and City Cores in EU (2018).

87. *Jeremy Azzopardi*: Effect of distance measures and feature representations on distance-based accessibility measures (2018).

88. *Patrick Kabatha*: An open source web GIS tool for analysis and visualization of elephant GPS telemetry data, alongside environmental and anthropogenic variables (2018).

89. *Richard Alphonce Giliba*: Effects of Climate Change on Potential Geographical Distribution of Prunus africana (African cherry) in the Eastern Arc Mountain Forests of Tanzania (2018).

90. *Eiður Kristinn Eiðsson*: Transformation and linking of authoritative multi-scale geodata for the Semantic Web: A case study of Swedish national building data sets (2018).

91. *Niamh Harty*: HOP!: a PGIS and citizen science approach to monitoring the condition of upland paths (2018).

92. *José Estuardo Jara Alvear*: Solar photovoltaic potential to complement hydropower in Ecuador: A GIS-based framework of analysis (2018).

93. *Brendan O'Neill*: Multicriteria Site Suitability for Algal Biofuel Production Facilities (2018).

94. *Roman Spataru*: Spatial-temporal GIS analysis in public health – a case study of polio disease (2018).

95. *Alicja Miodońska*: Assessing evolution of ice caps in Suðurland, Iceland, in years 1986 - 2014, using multispectral satellite imagery (2019).

96. *Dennis Lindell Schettini*: A Spatial Analysis of Homicide Crime's Distribution and Association with Deprivation in Stockholm Between 2010-2017 (2019).

97. *Damiano Vesentini*: The Po Delta Biosphere Reserve: Management challenges and priorities deriving from anthropogenic pressure and sea level rise (2019).

98. *Emilie Arnesten*: Impacts of future sea level rise and high water on roads, railways and environmental objects: a GIS analysis of the potential effects of increasing sea levels and highest projected high water in Scania, Sweden (2019).

99. *Syed Muhammad Amir Raza*: Comparison of geospatial support in RDF stores: Evaluation for ICOS Carbon Portal metadata (2019).

100. *Hemin Tofiq*: Investigating the accuracy of Digital Elevation Models from UAV images in areas with low contrast: A sandy beach as a case study (2019).

101. *Evangelos Vafeiadis*: Exploring the distribution of accessibility by public transport using spatial analysis. A case study for retail concentrations and public hospitals in Athens (2019).

102. *Milan Sekulic*: Multi-Criteria GIS modelling for optimal alignment of roadway by-passes in the Tlokweng Planning Area, Botswana (2019).

103. *Ingrid Piirisaar*: A multi-criteria GIS analysis for siting of utility-scale photovoltaic solar plants in county Kilkenny, Ireland (2019).

104. *Nigel Fox*: Plant phenology and climate change: possible effect on the onset of various wild plant species' first flowering day in the UK (2019).

105. *Gunnar Hesch*: Linking conflict events and cropland development in Afghanistan, 2001 to 2011, using MODIS land cover data and Uppsala Conflict Data Programme (2019).

106. *Elijah Njoku*: Analysis of spatial-temporal pattern of Land Surface Temperature (LST) due to NDVI and elevation in Ilorin, Nigeria (2019).

107. *Katalin Bunyevácz*: Development of a GIS methodology to evaluate informal urban green areas for inclusion in a community governance program (2019).

108. *Paul dos Santos*: Automating synthetic trip data generation for an agent-based simulation of urban mobility (2019).

109. *Robert O' Dwyer*: Land cover changes in Southern Sweden from the mid-Holocene to present day: Insights for ecosystem service assessments (2019).

110. *Daniel Klingmyr*: Global scale patterns and trends in tropospheric NO2 concentrations (2019).

111. *Marwa Farouk Elkabbany*: Sea Level Rise Vulnerability Assessment for Abu Dhabi, United Arab Emirates (2019).

112. *Jip Jan van Zoonen*: Aspects of Error Quantification and Evaluation in Digital Elevation Models for Glacier Surfaces (2020).

113. *Georgios Efthymiou*: The use of bicycles in a mid-sized city – benefits and obstacles identified using a questionnaire and GIS (2020).

114. *Haruna Olayiwola Jimoh*: Assessment of Urban Sprawl in MOWE/IBAFO Axis of Ogun State using GIS Capabilities (2020).

115. *Nikolaos Barmpas Zachariadis*: Development of an iOS, Augmented Reality for disaster management (2020).

116. *Ida Storm*: ICOS Atmospheric Stations: Spatial Characterization of CO2 Footprint Areas and Evaluating the Uncertainties of Modelled CO2 Concentrations (2020).

117. *Alon Zuta*: Evaluation of water stress mapping methods in vineyards using airborne thermal imaging (2020).

118. *Marcus Eriksson*: Evaluating structural landscape development in the municipality Upplands-Bro, using landscape metrics indices (2020).

119. *Ane Rahbek Vierø*: Connectivity for Cyclists? A Network Analysis of Copenhagen's Bike Lanes (2020).

120. *Cecilia Baggini*: Changes in habitat suitability for three declining Anatidae species in saltmarshes on the Mersey estuary, North-West England (2020).

121. *Bakrad Balabanian*: Transportation and Its Effect on Student Performance (2020).

122. *Ali Al Farid*: Knowledge and Data Driven Approaches for Hydrocarbon Microseepage Characterizations: An Application of Satellite Remote Sensing (2020).

123. *Bartlomiej Kolodziejczyk*: Distribution Modelling of Gene Drive-Modified Mosquitoes and Their Effects on Wild Populations (2020).

124. *Alexis Cazorla*: Decreasing organic nitrogen concentrations in European water bodies - links to organic carbon trends and land cover (2020).

125. *Kharid Mwakoba*: Remote sensing analysis of land cover/use conditions of community-based wildlife conservation areas in Tanzania (2021).

126. *Chinatsu Endo*: Remote Sensing Based Pre-Season Yellow Rust Early Warning in Oromia, Ethiopia (2021).

127. *Berit Mohr*: Using remote sensing and land abandonment as a proxy for long-term human out-migration. A Case Study: Al-Hassakeh Governorate, Syria (2021).

128. *Kanchana Nirmali Bandaranayake*: Considering future precipitation in delineation locations for water storage systems - Case study Sri Lanka (2021).

129. *Emma Bylund*: Dynamics of net primary production and food availability in the aftermath of the 2004 and 2007 desert locust outbreaks in Niger and Yemen (2021).

130. *Shawn Pace*: Urban infrastructure inundation risk from permanent sea-level rise scenarios in London (UK), Bangkok (Thailand) and Mumbai (India): A comparative analysis (2021).

131. *Oskar Evert Johansson*: The hydrodynamic impacts of Estuarine Oyster reefs, and the application of drone technology to this study (2021).

132. *Pritam Kumarsingh*: A Case Study to develop and test GIS/SDSS methods to assess the production capacity of a Cocoa Site in Trinidad and Tobago (2021).

133. *Muhammad Imran Khan*: Property Tax Mapping and Assessment using GIS (2021).

134. *Domna Kanari*: Mining geosocial data from Flickr to explore tourism patterns: The case study of Athens (2021).

135. *Mona Tykesson Klubien*: Livestock-MRSA in Danish pig farms (2021).

136. *Ove Njøten*: Comparing radar satellites. Use of Sentinel-1 leads to an increase in oil spill alerts in Norwegian waters (2021).

137. *Panagiotis Patrinos*: Change of heating fuel consumption patterns produced by the economic crisis in Greece (2021).

138. *Lukasz Langowski*: Assessing the suitability of using Sentinel-1A SAR multi-temporal imagery to detect fallow periods between rice crops (2021).

139. *Jonas Tillman*: Perception accuracy and user acceptance of legend designs for opacity data mapping in GIS (2022).

140. *Gabriela Olekszyk*: ALS (Airborne LIDAR) accuracy: Can potential low data quality of ground points be modelled/detected? Case study of 2016 LIDAR capture over Auckland, New Zealand (2022).

141. *Luke Aspland*: Weights of Evidence Predictive Modelling in Archaeology (2022).

142. *Luís Fareleira Gomes*: The influence of climate, population density, tree species and land cover on fire pattern in mainland Portugal (2022).

143. *Andreas Eriksson*: Mapping Fire Salamander (Salamandra salamandra) Habitat Suitability in Baden-Württemberg with Multi-Temporal Sentinel-1 and Sentinel-2 Imagery (2022).

144. *Lisbet Hougaard Baklid*: Geographical expansion rate of a brown bear population in Fennoscandia and the factors explaining the directional variations (2022).

145. *Victoria Persson*: Mussels in deep water with climate change: Spatial distribution of mussel (Mytilus galloprovincialis) growth offshore in the French Mediterranean with respect to climate change scenario RCP 8.5 Long Term and Integrated Multi-Trophic Aquaculture (IMTA) using Dynamic Energy Budget (DEB) modelling (2022).

146. *Benjamin Bernard Fabien Gérard Borgeais*: Implementing a multi-criteria GIS analysis and predictive modelling to locate Upper Palaeolithic decorated caves in the Périgord noir, France (2022).

147. *Bernat Dorado-Guerrero*: Assessing the impact of post-fire restoration interventions using spectral vegetation indices: A case study in El Bruc, Spain (2022).

148. *Ignatius Gabriel Aloysius Maria Perera*: The Influence of Natural Radon Occurrence on the Severity of the COVID-19 Pandemic in Germany: A Spatial Analysis (2022).

149. *Mark Overton*: An Analysis of Spatially-enabled Mobile Decision Support Systems in a Collaborative Decision-Making Environment (2022).

150. *Viggo Lunde*: Analysing methods for visualizing time-series datasets in open-source web mapping (2022).

151. *Johan Viscarra Hansson*: Distribution Analysis of Impatiens glandulifera in Kronoberg County and a Pest Risk Map for Alvesta Municipality (2022).

152. *Vincenzo Poppiti*: GIS and Tourism: Developing strategies for new touristic flows after the Covid-19 pandemic (2022).

153. *Henrik Hagelin*: Wildfire growth modelling in Sweden - A suitability assessment of available data (2023).

154. *Gabriel Romeo Ferriols Pavico*: Where there is road, there is fire (influence): An exploratory study on the influence of roads in the spatial patterns of Swedish wildfires of 2018 (2023).

155. *Colin Robert Potter*: Using a GIS to enable an economic, land use and energy output comparison between small wind powered turbines and large-scale wind farms: the case of Oslo, Norway (2023).

156. *Krystyna Muszel*: Impact of Sea Surface Temperature and Salinity on Phytoplankton blooms phenology in the North Sea (2023).

157. *Tobias Rydlinge*: Urban tree canopy mapping - an open source deep learning approach (2023).

158. *Albert Wellendorf*: Multi-scale Bark Beetle Predictions Using Machine Learning (2023).

159. *Manolis Papadakis*: Use of Satellite Remote Sensing for Detecting Archaeological Features: An Example from Ancient Corinth, Greece (2023).

160. *Konstantinos Sourlamtas*: Developing a Geographical Information System for a water and sewer network, for monitoring, identification and leak repair - Case study: Municipal Water Company of Naoussa, Greece (2023).

161. *Xiaoming Wang*: Identification of restoration hotspots in landscape-scale green infrastructure planning based on model-predicted connectivity forest (2023).

162. *Sarah Sienaert*: Usability of Sentinel-1 C-band VV and VH SAR data for the detection of flooded oil palm (2023).

163. *Katarina Ekeroot*: Uncovering the spatial relationships between Covid-19 vaccine coverage and local politics in Sweden (2023).

164. *Nikolaos Kouskoulis*: Exploring patterns in risk factors for bark beetle attack during outbreaks triggered by drought stress with harvester data on attacked trees: A case study in Southeastern Sweden (2023).

165. *Jonas Almén*: Geographic polarization and clustering of partisan voting: A local-level analysis of Stockholm Municipality (2023).

166. *Sara Sharon Jones*: Tree species impact on Forest Fire Spread Susceptibility in Sweden (2023).

167. *Takura Matswetu*: Towards a Geographic Information Systems and Data-Driven Integration Management. Studying holistic integration through spatial accessibility of services in Tampere, Finland. (2023).

168. *Duncan Jones*: Investigating the influence of the tidal regime on harbour porpoise *Phocoena phocoena* distribution in Mount's Bay, Cornwall (2023).

169. *Jason Craig Joubert*: A comparison of remote sensed semi-arid grassland vegetation anomalies detected using MODIS and Sentinel-3, with anomalies in ground-based eddy covariance flux measurements (2023).

170. *Anastasia Sarelli*: Land cover classification using machine-learning techniques applied to fused multi-modal satellite imagery and time series data (2024).

171. *Athanasios Senteles*: Integrating Local Knowledge into the Spatial Analysis of Wind Power: The case study of Northern Tzoumerka, Greece (2024).

172. *Rebecca Borg:* Using GIS and satellite data to assess access of green area for children living in growing cities (2024).

173. *Panagiotis–Dimitrios Tsachageas*: Multicriteria Evaluation in Real Estate Land-use Suitability Analysis: The case of Volos, Greece (2024).

174. *Hugo Nilsson*: Inferring lane-level topology of signalised intersections from aerial imagery and OpenStreetMap using deep learning (2024).

175. *Pavlos Alexantonakis*: Estimating lake water volume fluctuations using Sentinel-2 and ICESat-2 remote sensing data (2024).

176. *Karl-Martin Wigen*: Physical barriers and where to find them (2024).

177. *Martin Storsnes*: Temporal RX-algorithm performance on Sentinel-2 images (2024).

178. *Saulė Gabrielė Petraitytė*: The Relation Between Covid-19 Vaccination and Voting Trends in Lithuania: A Spatial Analysis (2024).

179. *Pedro Martinez Duran*: Olive yield forecasting from remote sensing and climate datasets in the Jaen province (Spain) (2024).

180. *Josefine Kynde Hämberg*: Proximity to Urban Green Spaces for Older Adults in Specific Housings - a Case Study of Malmö, Sweden (2024).

181. *Max Bengtsson*: A Site Selection of An Energy Island in the North Sea: Optimal Location in an Ecological and an Economic Scenario Using a Multicriteria Decision Analysis (MCDA) (2024).

182. *Anna Börmann*: Assessing Great Britain as a relocation site for the threatened Iberian Lynx in a changing climate (2024).

183. *Josephine Roosli*: Flood Risk Assessment for the Kävlinge River for Present and Future Climate Scenarios using HEC-RAS Rain-on-Grid (2024).

184. *Seán Flanagan*: Spatiotemporal dynamics of E-scooter sharing ridership and their associations with the built environment: A Swedish comparative study (2024).

185. *Wouter Vorsters*: Assessing the Impact of Combined Sewer Overflow on the Habitat of Lampetra planeri: A Case Study in Flanders, Belgium (2025).

186. *Kathleen Macdonald*: Cetacean strandings on the Scottish coast: coastal accessibility factors lead to underreporting (2025).

187. *Athanasios Emmanouil Mourampetzis*: Navigating the Shadows: A Comparative Analysis of SAR and Optical Imagery for Detecting (Dark) Vessels (2025).

188. *Nizam-ud-Din*: Spatial Land Records System using Geospatial Techniques: a case study of a Mid-Sized Village in Pakistan (2025).

189. *Nedim Nasic Kjellgren*: Linked Geodata: Improving Rooftop Photovoltaic Production Estimates through BIM-GIS Integration using Semantic Web Technologies (2025).

190. *Vedrana Pretkovic*: Spatio-temporal vegetation changes in the Pacific-Chocó region of Colombia during the conflict and post-conflict periods (2025).

191. *Evelina Bengtsson*: A Socioeconomic Dimension of Crime: A Spatial Study of Firearm-related Violence in Malmö (2025).

192. *Martynas Bielinis*: Application of C-band Radar Interferometry for Dune Monitoring in the Curonian Spit (2025).

193. *Paulina Magdalena Rieke*: Case study of the benefits of BIM and GIS solutions used on a live infrastructure project (2025).

194. *Alina Schärer*: Evaluating the Impact of Urban Green Spaces and Vegetation Characteristics on Land Surface Temperature Across Swiss Cities Using Machine Learning (2025).

195. *Paul Stewart:* Where is wild in Glasgow's Southside? A test of the applicability of relative wildness mapping to suburban Scotland (2025).

196. *Georgios Fylakis:* Spatiotemporal analysis of the integration between shared e-scooters and public transport: Case studies in Oslo and Stockholm (2025).

197. *Andreas Klasson*: Generating 3D building models according to Swedish building specification using footprints and airborne laser scanning (2025).

198. *Agaton Järemo Lawin*: The spread of Japanese knotweed in Scania: Invasion suitability prediction using species distribution modelling (2025).

199. *Jesse Stewart:* Contextualizing the Geographic Influence on Infantry Manoeuvrability in a Historical Battlefield Using GIS: A Case Study of the Canadian Corps in the Second Battle of Passchendaele, First World War (2025).

200. *Oskar Vejkdal Thorsberg*: Automatic geometry extraction in digital building permits: A case study using BIM and NS Building (2025).

201. *Spyridon Gerafentis*: Impact of the COVID-19 "Lockdown" on Air Quality in Athens (2025).

202. *Symeon Andriotis*: Political Violence in Athens, Greece (2008-2024): A Machine Learning Approach for Predictive Modelling of Spatial Risk Patterns (2025).

203. *Simon Westman*: Detecting Structurally Old Scots Pine: A Crown-Metric Approach Using National ALS and LIFT Enrichment (2026).

204. *Freja Randeris Kristoffersen*: Satellite-Derived Bathymetry of Danish Coastal Waters Using Machine Learning with Sentinel-2 and ICESat-2 data (2026).

205. *Markus Honkanen*: Securitas Per Scientiam: GIS-MCDA of Civil Defence Shelter Distribution Efficiency in the Helsinki Capital Region (2026).

206. *Amanda Carolina Santos Motta*: Visualization Tools for Simulation Results Based on 3D City Models: An Urban Planner-Focused Study (2026).

207. *Gintars Krumins*: Mapping forest felling activities in Latvia from Sentinel-2 satellite imagery using machine learning (2026).